

AD-A067 867

PENNSYLVANIA STATE UNIV UNIVERSITY PARK APPLIED RESE--ETC F/G 20/4
FOURTH-ORDER KELLER BOX SOLUTION OF THE INCOMPRESSIBLE AXISYMMETRIC (U)
FEB 79 J M CIMBALA
N00024-79-C-6043
NL

UNCLASSIFIED

1 OF 1
AD
A067 867



LEVEL

(12)
B.S.

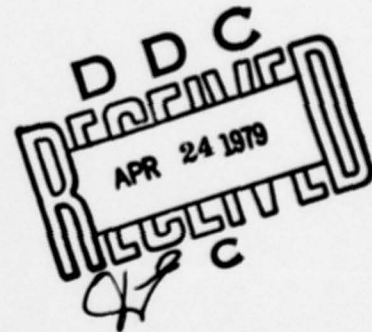
AD A067867

FOURTH-ORDER KELLER BOX SOLUTION OF THE
INCOMPRESSIBLE AXISYMMETRIC BOUNDARY
LAYER EQUATIONS

J. M. Cimbala

Technical Memorandum
File No. TM 79-18
February 2, 1979
Contract No. N00024-79-C-6043

Copy No. 39



DDC FILE COPY

The Pennsylvania State University
APPLIED RESEARCH LABORATORY
Post Office Box 30
State College, PA 16801

Approved for Public Release
Distribution Unlimited

NAVY DEPARTMENT

NAVAL SEA SYSTEMS COMMAND

391007

79 04 20 023

UNCLASSIFIED

SECURITY CLASSIFICATION OF THIS PAGE (When Data Entered)

14
ARL/PSU

REPORT DOCUMENTATION PAGE

READ INSTRUCTIONS
BEFORE COMPLETING FORM

1. REPORT NUMBER

2. GOVT ACCESSION NO.

3. RECIPIENT'S CATALOG NUMBER

7 TM-79-18

4. TITLE (and Subtitle)

5. TYPE OF REPORT & PERIOD COVERED

FOURTH-ORDER KELLER BOX SOLUTION OF THE
INCOMPRESSIBLE AXISYMMETRIC BOUNDARY
LAYER EQUATIONS

Technical Memorandum

6. AUTHOR(s)

7. PERFORMING ORG. REPORT NUMBER

N60024-79-C-6043

8. CONTRACT OR GRANT NUMBER(s)

10 J. M. Cimbal

9. PERFORMING ORGANIZATION NAME AND ADDRESS

Applied Research Laboratory
Post Office Box 30
State College, PA 1680110. PROGRAM ELEMENT, PROJECT, TASK
AREA & WORK UNIT NUMBERS

11. CONTROLLING OFFICE NAME AND ADDRESS

Naval Sea Systems Command
Code NSEA-0351
Washington, DC 20362

12. REPORT DATE

February 1979

13. NUMBER OF PAGES

60

14. MONITORING AGENCY NAME & ADDRESS (if different from Controlling Office)

15. SECURITY CLASS. (of this report)

UNCLASSIFIED

15a. DECLASSIFICATION/DOWNGRADING
SCHEDULE

16. DISTRIBUTION STATEMENT (of this Report)

Approved for public release. Distribution unlimited.
Per NAVSEA - 4 April 1979

17. DISTRIBUTION STATEMENT (of the abstract entered in Block 20, if different from Report)

18. SUPPLEMENTARY NOTES

This material is to be presented at the AIAA Student Paper Competition,
April 20-21, 1979 at West Virginia University.

19. KEY WORDS (Continue on reverse side if necessary and identify by block number)

boundary layer
incompressible flow
Keller box solution

20. ABSTRACT (Continue on reverse side if necessary and identify by block number)

A computer code has been written for a general finite difference solution
procedure of the incompressible boundary layer equations on a body of
revolution. The procedure, a fourth-order accurate extension of Keller's
Box Method, is capable of treating laminar or turbulent boundary layers up to
a separation point and includes transverse curvature effects. The analysis
has been coded for the Penn State IBM 370/3033 computer and has been shown
to provide solutions comparable in accuracy to similar second-order schemes

DD FORM 1 JAN 73 1473

EDITION OF 1 NOV 65 IS OBSOLETE

UNCLASSIFIED

SECURITY CLASSIFICATION OF THIS PAGE (When Data Entered)

79 04

391007
20 023next
page
JB

UNCLASSIFIED

SECURITY CLASSIFICATION OF THIS PAGE(When Data Entered)

but with fewer grid points and with less computer time. Results and comparisons with both experiment and second-order methods are presented in graphical form for a low-drag body of revolution.

UNCLASSIFIED

SECURITY CLASSIFICATION OF THIS PAGE(When Data Entered)

| | |
|---------------------------------|---|
| ACCESSION for | |
| NTIS | White Section <input checked="" type="checkbox"/> |
| DOC | Buff Section <input type="checkbox"/> |
| UNANNOUNCED | |
| JUSTIFICATION | |
| DISTRIBUTION/AVAILABILITY CODES | |
| CIAL | |
| A | |

Subject: Fourth-Order Keller Box Solution of the Incompressible Axisymmetric Boundary Layer Equations

References: See page 25

Abstract: A computer code has been written for a general finite difference solution procedure of the incompressible boundary layer equations on a body of revolution. The procedure, a fourth-order accurate extension of Keller's Box Method, is capable of treating laminar or turbulent boundary layers up to a separation point and includes transverse curvature effects. The analysis has been coded for the Penn State IBM 370/3033 computer and has been shown to provide solutions comparable in accuracy to similar second-order schemes but with fewer grid points and with less computer time. Results and comparisons with both experiment and second-order methods are presented in graphical form for a low-drag body of revolution.

Acknowledgment: This work was sponsored by Naval Sea Systems Command, Code NSEA-0351.

Table of Contents

| | <u>Page</u> |
|---|-------------|
| Abstract | 1 |
| Acknowledgment | 1 |
| Nomenclature | 3 |
| List of Figures | 5 |
| Dimensional Reference Quantities | 6 |
| INTRODUCTION | 7 |
| INCOMPRESSIBLE BOUNDARY LAYER EQUATIONS | 8 |
| DEVELOPMENT OF FOURTH-ORDER BOX EQUATIONS | 11 |
| MATRIX FORMULATION AND SOLUTION | 15 |
| RESULTS | 18 |
| Integral Parameters | 20 |
| Boundary Layer Profiles | 22 |
| Computer Run Times | 22 |
| CONCLUDING REMARKS | 23 |
| References | 25 |
| Appendix A: Algebraic Eddy Viscosity Model | 26 |
| Inner Region | 26 |
| Outer Region | 28 |
| Transition Region | 29 |
| Appendix B: Differentiation of Vector \vec{g}' | 30 |
| Inner Region | 30 |
| Outer Region | 31 |
| Appendix C: Derivation of Finite-Difference Expressions | 32 |
| Appendix D: Block Tridiagonal Matrix Solution | 43 |
| Figures | 50 |

Nomenclature

$$C_{f_{\infty}} - \text{wall skin friction coefficient} = \frac{2\tau_w^*}{\rho^* U_{\infty}^{*2}}$$

$$\epsilon - \text{turbulent eddy viscosity} = \frac{\rho^* \epsilon^*}{\mu^*}$$

$$p - \text{static pressure} = \frac{p^*}{\rho^* U_{\infty}^{*2}}$$

$$\phi - \text{body surface angle, see Figure 1}$$

$$\psi - \text{Stokes stream function} = \frac{\psi^*}{\rho^* L^* U_{\infty}^*}$$

$$r - \text{distance normal from centerline} = \frac{r^*}{L^*}$$

$$r_o - \text{body radius} = \frac{r_o^*}{L^*}$$

$$Re - \text{Reynolds number} = \frac{\rho^* U^* L_{\infty}^*}{\mu^*}$$

$$u - \text{velocity component in x-direction} = \frac{u^*}{U_{\infty}^*}$$

$$u_e - \text{inviscid velocity at body surface} = \frac{u_e^*}{U_{\infty}^*}$$

Nomenclature (Continued)

$$\overline{-u'v'} \quad - \quad \text{Reynolds stress in boundary layer} = \frac{\rho^* (\overline{u'v'})^*}{\rho^* U_\infty^{*2}}$$

$$x \quad - \quad \text{arc length distance along body} = \frac{x^*}{L^*}$$

$$y \quad - \quad \text{distance normal to body surface} = \frac{y^*}{L^*}$$

Other quantities are defined in the text.

List of Figures

| <u>Figure</u> | <u>Title</u> | <u>Page</u> |
|---------------|--|-------------|
| 1 | Coordinate System for Body of Revolution | 50 |
| 2 | Box Element for Finite Difference Approximation | 51 |
| 3 | F-57 Body Geometry | 52 |
| 4 | Pressure Distribution, F-57 Body, $Re = 1.2 \times 10^6$ | 53 |
| 5 | Wall Friction Coefficient, F-57 Body, $Re = 1.2 \times 10^6$ | 54 |
| 6 | Momentum Area Deficit, F-57 Body, $Re = 1.2 \times 10^6$ | 55 |
| 7 | Boundary Layer Shape Factor, F-57 Body, $Re = 1.2 \times 10^6$ | 56 |
| 8 | Mean Velocity Profile at $x_o = 0.601$, F-57 Body | 57 |
| 9 | Mean Velocity Profile at $x_o = 0.880$, F-57 Body | 58 |
| 10 | Mean Velocity Profile at $x_o = 0.990$, F-57 Body | 59 |

Dimensional Reference Quantities

L^* - reference length

μ^* - viscosity

ν^* - kinematic viscosity

ρ^* - density

τ_w^* - wall shear stress = $\mu^* \left(\frac{\partial u^*}{\partial y^*} \right)_w$

u_τ^* - friction velocity = $\left(\frac{\tau_w^*}{\rho^*} \right)$

U_∞^* - free stream velocity

INTRODUCTION

A second-order accurate Keller box solution of the incompressible axisymmetric boundary layer equations has been employed by Cebeci [1] using the Mangler-Levy-Lees transformation to avoid a singularity at the stagnation point. Unfortunately this transformation causes a singularity at the tail of the body making extension of the calculations into the wake region impossible.

A second-order accurate code has been written by Hoffman [6] which uses non-transformed variables to solve the equations. This code is incapable of starting at the stagnation point; therefore a complete boundary layer profile must be input from the Cebeci program mentioned above. With the untransformed variables the singularity at the tail point is eliminated and better accuracy in the solution is obtained near the tail.

The fourth-order Keller box method is a natural extension of the second-order scheme presently employed by Hoffman [6]. The term fourth-order as used here refers to the truncation error in the coordinate normal to the axisymmetric body surface. The truncation error in the tangential coordinate is still second-order. The fourth-order scheme also uses the non-transformed variables mentioned above and is set up to accept a boundary layer profile from the Cebeci program at a station downstream of the stagnation point in the same way as the method of Hoffman. A fourth-order solution provides higher accuracy everywhere for the same mesh spacing or provides the same accuracy for a larger mesh spacing,

when compared to second-order solutions. Larger mesh spacing requires less computer time to obtain a solution; therefore the fourth-order solution can provide the same accuracy with less computer time in spite of the increased complexity over the second-order method.

INCOMPRESSIBLE BOUNDARY LAYER EQUATIONS

The boundary layer equations on a body of revolution for steady mean flow, including transverse curvature effects, are [1]:

$$\text{Continuity} \quad \frac{\partial}{\partial x} (ru) + \frac{\partial}{\partial y} (rv) = 0, \quad (1)$$

$$\text{Momentum} \quad u \frac{\partial u}{\partial x} + v \frac{\partial u}{\partial y} = -\frac{dp}{dx} + \frac{1}{r} \frac{\partial}{\partial y} \left[r \left(\frac{1}{Re} \frac{\partial u}{\partial y} - \overline{u'v'} \right) \right], \quad (2)$$

where dimensionless variables as defined in the nomenclature have been used and the coordinate system is shown in Figure 1. The boundary conditions are:

$$u(x, 0) = 0, \quad (3)$$

$$v(x, 0) = 0, \quad (4)$$

$$\lim_{y \rightarrow \infty} u(x, y) = u_e(x), \quad (5)$$

where $u_e(x)$ is the inviscid surface velocity.

It is assumed that the Reynolds stress is related to the velocity field by the relation

$$\overline{u'v'} = \frac{\epsilon}{Re} \frac{\partial u}{\partial y}, \quad (6)$$

where ϵ is the eddy viscosity. An algebraic eddy viscosity model is used and described in detail in Appendix A. Using Equation (6) the momentum equation becomes

$$u \frac{\partial u}{\partial x} + v \frac{\partial u}{\partial y} = - \frac{dp}{dx} + \frac{1}{r} \frac{\partial}{\partial y} \left[r(1 + \epsilon) \frac{\partial u}{\partial y} \right] . \quad (7)$$

The geometric relation between r and y from Figure 1 is:

$$r(x, y) = r_0(x) + y \cos \phi . \quad (8)$$

The term $y \cos \phi$ in Equation (8) is the transverse curvature term which is important at the aft end of the body where the boundary layer thickness is of the same order of magnitude as the body radius.

The Reynolds number is eliminated from Equation (7), in the case of a "thin" boundary layer, by introducing the scaled variables:

$$v = \frac{\bar{v}}{\sqrt{Re}} , \quad (9)$$

$$y = \frac{\bar{y}}{\sqrt{Re}} . \quad (10)$$

Equations (1), (7), and (8) become respectively,

$$\frac{\partial}{\partial x} (ru) + \frac{\partial}{\partial y} (r\bar{v}) = 0 , \quad (11)$$

$$u \frac{\partial u}{\partial x} + \bar{v} \frac{\partial u}{\partial \bar{y}} = \frac{dp}{dx} + \frac{1}{r} \frac{\partial}{\partial \bar{y}} \left[r(1 + \epsilon) \frac{\partial u}{\partial \bar{y}} \right] , \quad (12)$$

$$r(x, \bar{y}) = r_0(x) + \frac{\bar{y}}{\sqrt{Re}} \cos \phi . \quad (13)$$

In order to use the box method, these equations must be rewritten in first-order form. The Stokes stream function is introduced, defined by

$$ru = \frac{\partial \psi}{\partial y} \quad , \quad r\bar{v} = \frac{-\partial \psi}{\partial x} \quad . \quad (14)$$

The continuity equation, Equation (11), is identically satisfied by the stream function. The Euler equation at the body surface which relates the pressure gradient to the inviscid surface velocity is:

$$\frac{dp}{dx} = -u_e \frac{du_e}{dx} \quad . \quad (15)$$

If use is made of the laminar shear stress, defined by

$$\tau = \frac{\partial u}{\partial y} \quad , \quad (16)$$

then the momentum equation, Equation (12), can be written in the following first-order form:

$$\frac{r}{2} \frac{\partial}{\partial x} (u^2 - u_e^2) - \frac{\partial \psi}{\partial x} \tau - \frac{\partial}{\partial y} (rb\tau) = 0 \quad , \quad (17)$$

where

$$b = 1 + \epsilon \quad . \quad (18)$$

Summarizing, the set of first-order equations to be solved is:

$$\frac{\partial}{\partial y} (rb) = \frac{r}{2} \frac{\partial}{\partial x} (u^2 - u_e^2) - \frac{\partial \psi}{\partial x} \tau \quad , \quad (19)$$

$$\frac{\partial}{\partial y} (\psi) = ru \quad , \quad (20)$$

$$\frac{\partial}{\partial y} (u) = \tau \quad . \quad (21)$$

The new boundary conditions become [6],

$$u = \psi = 0 \quad \text{at} \quad \bar{y} = 0, \quad (22)$$

$$u \rightarrow u_e \quad \text{as} \quad \bar{y} \rightarrow \infty. \quad (23)$$

DEVELOPMENT OF FOURTH-ORDER EQUATIONS

The finite-difference procedure used in solving the parabolic boundary layer equations is the box method of H. B. Keller [2]. The first-order form of the governing differential equations, (19)-(21), when put in finite difference form will result in algebraic equations which relate unknowns along line (i+1), as shown in Figure 2, to line i. The solution along line i is assumed known and since the equations are parabolic the solution at line (i+1) can be obtained. The result is a marching procedure beginning at the initial station and proceeding downstream.

In applying Keller's box method one approximates the equations by difference quotients about point P, the geometric center of the box element, as shown in Figure 2. The derivatives in the axial direction are second-order accurate and are given by simple centered differences. The fourth-order accurate expression used for derivatives in the normal coordinate is given by Wornom [3] as

$$\bar{g}_{j+1} - \bar{g}_j - \frac{h_j}{2} \left(\bar{g}_{j+1}' + \bar{g}_j' \right) + \frac{h_j^2}{12} \left(\bar{g}_{j+1}'' - \bar{g}_j'' \right) + O(h_j^5) = 0, \quad (24)$$

where primes denote differentiation in the normal direction (w.r.t. \bar{y}) and h_j is the step-size in the normal direction given by

$$h_j = \bar{y}_{j+1} - \bar{y}_j. \quad (25)$$

\vec{g} represents a matrix of the differentiable quantities from Equations (19)-(21) given by

$$\vec{g}' = \begin{bmatrix} r b \tau \\ \psi \\ u \end{bmatrix} . \quad (26)$$

From these equations the first derivative of \vec{g} is obviously

$$\vec{g}' = \begin{bmatrix} -\frac{\partial \psi}{\partial x} \tau + \frac{r}{2} \frac{\partial}{\partial x} (u^2 - u_e^2) \\ ru \\ \tau \end{bmatrix} . \quad (27)$$

The form of \vec{g}'' , however, is not so obvious, and becomes quite involved algebraically. In differentiating Equation (27) one obtains terms which contain the derivative τ' . Here the turbulence model used to determine the eddy viscosity ϵ becomes of great significance. In the inner region ϵ is given by

$$\epsilon = C_\epsilon |\tau| , \quad (28)$$

where

$$C_\epsilon = Re^{3/2} \ell^2 \frac{r}{r_0} , \quad (29)$$

and where ℓ is the mixing length, also a function of \bar{y} . In the outer region, however, ϵ is constant and independent of both \bar{y} and τ . See Appendix A for a more detailed description of the turbulence model.

The derivative τ' may be determined from Equation (19) by using the product rule of differentiation and isolating τ' . In the outer region

the value of b from Equation (18) is constant and is left as such. However, in the inner region the value of b is a function of \bar{y} , and must also be differentiated. Thus the expression for τ' in the inner region becomes much more complicated than that in the outer region. Appendix B shows the derivation of \hat{g}'' for both of these cases, the results of which appear below:

$$\hat{g}'' \text{ inner} = \left[\begin{array}{c} \left\{ -\tau \frac{\partial}{\partial x} (ru) + (ru) \frac{\partial \tau}{\partial x} + \frac{\alpha}{2} \frac{\partial}{\partial x} (u^2 - u_e^2) - \frac{\partial \psi}{\partial x} \left(\frac{1}{1+2s\tau} \right) \cdot \right. \\ \left. \left[\frac{1}{2} \frac{\partial}{\partial x} (u^2 - u_e^2) - \frac{\tau}{r} \frac{\partial \psi}{\partial x} - s'\tau^2 - \frac{\alpha}{r} \tau - \frac{\alpha}{r} s\tau^2 \right] \right\} \\ \{ \alpha u + r\tau \} \\ \left\{ \left(\frac{1}{1+2s\tau} \right) \left[\frac{1}{2} \frac{\partial}{\partial x} (u^2 - u_e^2) - \frac{\tau}{r} \frac{\partial \psi}{\partial x} - s'\tau^2 - \frac{\alpha}{r} \tau - \frac{\alpha}{r} s\tau^2 \right] \right\} \end{array} \right] \quad (30)$$

$$\hat{g}'' \text{ outer} = \left[\begin{array}{c} \left\{ -\tau \frac{\partial}{\partial x} (ru) + (ru) \frac{\partial \tau}{\partial x} + \frac{\alpha}{2} \frac{\partial}{\partial x} (u^2 - u_e^2) - \frac{\partial \psi}{\partial x} \left(\frac{1}{rb} \right) \cdot \left[\frac{r}{2} \cdot \right. \right. \\ \left. \left. \frac{\partial}{\partial x} (u^2 - u_e^2) - \alpha b\tau - \tau \frac{\partial \psi}{\partial x} \right] \right\} \\ \{ \alpha u + r\tau \} \\ \left\{ \frac{1}{rb} \left[\frac{r}{2} \frac{\partial}{\partial x} (u^2 - u_e^2) - \alpha b\tau - \tau \frac{\partial \psi}{\partial x} \right] \right\} \end{array} \right] \quad (31)$$

Equations (26), (27), and either (30) or (31) are then substituted into the finite-difference expression, Equation (24) to obtain three nonlinear finite-difference equations. The $\frac{\partial}{\partial x} ()$ terms in these equations are approximated by

a central difference quotient, as already mentioned, making the equations second-order accurate in the x coordinate and fourth-order accurate in the \bar{y} coordinate. The non-linear terms are then linearized by Newton's method to obtain three linear finite-difference equations, developed in Appendix C, which are shown below:

$$\begin{aligned} & \hat{A1}_{i+1,j} \delta\psi_{i+1,j} + \hat{B1}_{i+1,j} \delta u_{i+1,j} + \hat{C1}_{i+1,j} \delta\tau_{i+1,j} \\ & + \hat{D1}_{i+1,j} \delta\psi_{i+1,j+1} + \hat{E1}_{i+1,j} \delta u_{i+1,j+1} + \hat{F1}_{i+1,j} \delta\tau_{i+1,j+1} = \hat{S1}_{i+1,j} , \end{aligned} \quad (32)$$

$$\begin{aligned} & \hat{A2}_{i+1,j} \delta\psi_{i+1,j} + \hat{B2}_{i+1,j} \delta u_{i+1,j} + \hat{C2}_{i+1,j} \delta\tau_{i+1,j} + \hat{D2}_{i+1,j} \delta\psi_{i+1,j+1} \\ & + \hat{E2}_{i+1,j} \delta u_{i+1,j+1} + \hat{F2}_{i+1,j} \delta\tau_{i+1,j+1} = \hat{S2}_{i+1,j} , \end{aligned} \quad (33)$$

$$\begin{aligned} & \hat{A3}_{i+1,j} \delta\psi_{i+1,j} + \hat{B3}_{i+1,j} \delta u_{i+1,j} + \hat{C3}_{i+1,j} \delta\tau_{i+1,j} + \hat{D3}_{i+1,j} \delta\psi_{i+1,j+1} \\ & + \hat{E3}_{i+1,j} \delta u_{i+1,j+1} + \hat{F3}_{i+1,j} \delta\tau_{i+1,j+1} = \hat{S3}_{i+1,j} . \end{aligned} \quad (34)$$

where the " δ " terms in the above equations indicate corrections to ψ , u , and τ . The appropriate boundary conditions become

$$\delta\psi_{i+1,1} = 0 , \quad (35)$$

$$\delta u_{i+1,1} = 0 , \quad (36)$$

$$\delta u_{i+1,N+1} = 0 . \quad (37)$$

MATRIX FORMULATION AND SOLUTION

In order to put the equations in tridiagonal matrix form, the boundary conditions given by Equations (35)-(37) and the finite-difference equations given by Equations (32)-(34) are grouped in the following fashion (i+1 subscripts are understood):

$$\left. \begin{aligned} \delta\psi_1 &= 0 \\ \delta u_1 &= 0 \\ \hat{A3}_1 \delta\psi_1 + \hat{B3}_1 \delta u_1 + \hat{C3}_1 \delta\tau_1 + \hat{D3}_1 \delta\tau_2 + \hat{E3}_1 \delta u_2 + \hat{F3}_1 \delta\tau_2 &= \hat{S3}_1 \end{aligned} \right\} 1^{st}$$

$$\left. \begin{aligned} \hat{A1}_1 \delta\psi_1 + \hat{B1}_1 \delta u_1 + \hat{C1}_1 \delta\tau_1 + \hat{D1}_1 \delta\psi_2 + \hat{E1}_1 \delta u_2 + \hat{F1}_1 \delta\tau_2 &= \hat{S1}_1 \\ \hat{A2}_1 \delta\psi_1 + \hat{B2}_1 \delta u_1 + \hat{C2}_1 \delta\tau_1 + \hat{D2}_1 \delta\psi_2 + \hat{E2}_1 \delta u_2 + \hat{F2}_1 \delta\tau_2 &= \hat{S2}_1 \\ \hat{A3}_2 \delta\psi_2 + \hat{B3}_2 \delta u_2 + \hat{C3}_2 \delta\tau_2 + \hat{D3}_2 \delta\psi_3 + \hat{E3}_2 \delta u_3 + \hat{F3}_2 \delta\tau_3 &= \hat{S2}_1 \end{aligned} \right\} 2^{nd}$$

$$\left. \begin{aligned} \hat{A1}_{j-1} \delta\psi_{j-1} + \hat{B1}_{j-1} \delta u_{j-1} + \hat{C1}_{j-1} \delta\tau_{j-1} + \hat{D1}_{j-1} \delta\psi_j + \hat{E1}_{j-1} \delta u_j + \hat{F1}_{j-1} \delta\tau_j &= \hat{S1}_{j-1} \\ \hat{A2}_{j-1} \delta\psi_{j-1} + \hat{B2}_{j-1} \delta u_{j-1} + \hat{C2}_{j-1} \delta\tau_{j-1} + \hat{D2}_{j-1} \delta\psi_j + \hat{E2}_{j-1} \delta u_j + \hat{F2}_{j-1} \delta\tau_j &= \hat{S2}_{j-1} \\ \hat{A3}_{j-1} \delta\psi_j + \hat{B3}_j \delta u_j + \hat{C3}_j \delta\tau_j + \hat{D3}_j \delta\psi_{j+1} + \hat{E3}_j \delta u_{j+1} + \hat{F3}_j \delta\tau_{j+1} &= \hat{S3}_j \end{aligned} \right\} j^{th}$$

$$\left. \begin{aligned} \hat{A1}_N \delta\psi_N + \hat{B1}_N \delta u_N + \hat{C1}_N \delta\tau_N + \hat{D1}_N \delta\psi_{N+1} + \hat{E1}_N \delta u_{N+1} + \hat{F1}_N \delta\tau_{N+1} &= \hat{S1}_N \\ \hat{A2}_N \delta\psi_N + \hat{B2}_N \delta u_N + \hat{C2}_N \delta\tau_N + \hat{D2}_N \delta\psi_{N+1} + \hat{E2}_N \delta u_{N+1} + \hat{F2}_N \delta\tau_{N+1} &= \hat{S2}_N \\ \delta u_{N+1} &= 0 \end{aligned} \right\} (N+1)^{th}$$

By defining a 3-component column vector Z_j according to

$$Z_j = \begin{bmatrix} \delta\psi \\ \delta u \\ \delta\tau \end{bmatrix}_j, \quad (38)$$

the preceding equations can be written as the following system of matrix equations:

$$A_1 Z_1 + C_1 Z_2 = R_1, \quad (39)$$

$$B_j Z_{j-1} + A_j Z_j + C_j Z_{j+1} = R_j, \quad 2 \leq j \leq N, \quad (40)$$

$$B_{N+1} Z_N + A_{N+1} Z_{N+1} = R_{N+1}, \quad (41)$$

where A_j , B_j , and C_j are 3×3 matrices as follows:

$$A_1 = \begin{bmatrix} 1 & 0 & 0 \\ 0 & 1 & 0 \\ \hat{A}_{31} & \hat{B}_{31} & \hat{C}_{31} \end{bmatrix}, \quad (42)$$

$$C_j = \begin{bmatrix} 0 & 0 & 0 \\ 0 & 0 & 0 \\ \hat{A}_{3j} & \hat{E}_{3j} & \hat{F}_{3j} \end{bmatrix}, \quad 1 \leq j \leq N, \quad (43)$$

$$B_j = \begin{bmatrix} \hat{A}_{1j-1} & \hat{B}_{1j-1} & \hat{C}_{1j-1} \\ \hat{A}_{2j-1} & \hat{B}_{2j-1} & \hat{C}_{2j-1} \\ 0 & 0 & 0 \end{bmatrix}, \quad 2 \leq j \leq N+1, \quad (44)$$

$$A_j = \begin{bmatrix} \hat{D}_{1j-1} & \hat{E}_{1j-1} & \hat{F}_{1j-1} \\ \hat{D}_{2j-1} & \hat{E}_{2j-1} & \hat{F}_{2j-1} \\ \hat{A}_{3j} & \hat{B}_{3j} & \hat{C}_{3j} \end{bmatrix}, \quad 2 \leq j \leq N, \quad (45)$$

$$A_{N+1} = \begin{bmatrix} \hat{D1}_N & \hat{E1}_N & \hat{F1}_N \\ \hat{D2}_N & \hat{E2}_N & \hat{F2}_N \\ 0 & 1 & 0 \end{bmatrix}, \quad (46)$$

and the R_j are 3-component column vectors as follows:

$$R_1 = \begin{bmatrix} 0 \\ 0 \\ S3_1 \end{bmatrix}, \quad (47)$$

$$R_j = \begin{bmatrix} \hat{S1}_{j-1} \\ \hat{S2}_{j-1} \\ \hat{S3}_j \end{bmatrix}, \quad (48)$$

and

$$R_{N+1} = \begin{bmatrix} \hat{S1}_N \\ \hat{S2}_N \\ 0 \end{bmatrix}. \quad (49)$$

Then Equations (39)-(41) can be written in the compact block matrix form:

$$A_t Z = R, \quad (50)$$

where A_t is an $(N+1) \times (N+1)$ block tridiagonal matrix given by

$$A_t = \begin{bmatrix} A_1 & C_1 & & & \\ B_2 & A_2 & C_2 & & 0 \\ & B_3 & A_3 & C_3 & \\ & & B_N & A_N & C_N \\ 0 & & & B_{N+1} & A_{N+1} \end{bmatrix}, \quad (51)$$

and \tilde{Z} and \tilde{R} are $(N+1)$ -component column vectors as follows

$$\tilde{Z} = \begin{bmatrix} Z_1 \\ Z_2 \\ | \\ | \\ | \\ Z_{N+1} \end{bmatrix}, \quad \tilde{R} = \begin{bmatrix} R_1 \\ R_2 \\ | \\ | \\ | \\ R_{N+1} \end{bmatrix}. \quad (52)$$

Because the coefficient matrix A_c is block tridiagonal, Equation (50) can be solved by an efficient elimination procedure similar to that used by Keller [10]. This procedure is presented in detail in Appendix D. The result is a solution for each of the correction terms $\delta\psi$, δu , and $\delta\tau$ in Equations (32)-(34).

These correction terms are then added to the values of $\psi_{i+1,j}$, $u_{i+1,j+1}$, etc., in order to obtain new iterates for these variables. The iteration procedure is continued until prescribed convergence tolerances are met.

RESULTS

In this paper computer solutions using the present fourth-order box method are compared to the second-order box solution of Hoffman [6] and with the experimental results of Patel and Lee [14] for a low drag body revolution. The body used was the F-57 body, shown in Figure 3; its

coordinates are given below [14]:

For $0 \leq x_0 \leq x_m$ (fore-body) ,

$$\frac{r_0}{r_m} = \left\{ -1.1723 \xi_1^4 + 0.7088 \xi_1^3 + 1.0993 \xi_1^2 + 0.3642 \xi_1 \right\}^{\frac{1}{2}} . \quad (53)$$

For $x_m \leq x_0 \leq 1$ (pointed aft-body) ,

$$\frac{r_0}{r_m} = \left\{ -0.11996 \xi_2^5 - 2.58278 \xi_2^4 + 3.52544 \xi_2^3 + 0.17730 \xi_2^2 \right\}^{\frac{1}{2}} , \quad (54)$$

where $\xi_1 = x_0/x_m$, $\xi_2 = (1 - x_0)/(1 - x_m)$, x_0 is the axial distance measured from the nose, r_0 is the local radius, x_m is the axial location of the maximum radius r_m , and all length variables have been non-dimensionalized with respect to L^* , the body length ($L^* = 1.219m$). Thus, $x_m = x_m^*/L^* = 0.4446$, $r_m = r_m^*/L^* = 0.1170$. All solutions were at a Reynolds number of 1.2×10^6 where $Re = \frac{U_\infty^* L^*}{\nu^*}$. The experimental measurements [14] were taken with the boundary layer tripped at $x_0 = x_0^*/L^* = 0.475$ by a circular trip wire of 1.664 mm diameter wrapped around the body. Subsequent analysis of data revealed that the downstream influence of such a relatively large trip wire may have persisted up to $x_0 = 0.6$ [14]. The turbulence model used in the computer code cannot accurately simulate such a sudden jump from laminar to turbulent flow; thus a transition intermittency factor has been included as described in Appendix A. The axial distance where the transition region should begin in the computer solution was then chosen

by equating the momentum deficit area of the calculation to that of the experiment. Following Hoffman [11] an axial station at $x_0 = 0.3271$ was used in the calculations.

The pressure distribution input to the computer programs was taken from the strong-interaction calculations of Hoffman [11]. The iterative procedure used to generate these data is based on a correction of the displacement body idea to represent streamline curvature effects by means of a simple pressure mapping, and is described in Reference 11. Figure 4 shows this distribution as a function of the axial body coordinate.

As mentioned previously, in order to avoid a singularity at the nose point, the computer codes for both the second- and fourth-order box solutions, which use non-transformed variables, are set up to accept as input a boundary layer profile at some station downstream of the nose. The station was chosen in the laminar region at $x_0 = 0.09548$ and the profile was generated with Hoffman's second-order computer solution which uses the Mangler-Levy-Lees transformation [6].

Integral Parameters

Calculations were made of the integral parameters C_f , Θ , and H at each axial coordinate x_0 where Θ is the momentum flux deficit,

$$\Theta = \int_0^{\infty} \frac{u}{u_e} \left(1 - \frac{u}{u_e} \right) r \, dy \quad , \quad (55)$$

H is the boundary layer shape factor,

$$H = \frac{\delta^*}{\theta} , \quad (56)$$

δ^* is the mass flux deficit

$$\delta^* = \int_0^{\infty} \left(1 - \frac{u}{u_e} \right) r \, dy , \quad (57)$$

and C_f is the wall friction coefficient,

$$C_f = \frac{2\tau_w}{\rho u_e} . \quad (58)$$

Results are presented in graphical form in Figures 5-7 for C_f , θ , and H, respectively, as functions of x_0 . The fourth-order calculations, which start with an input boundary layer profile of 11 points in the normal coordinate at an axial station of $x_0 = 0.09548$, are compared with the second-order calculations [6], starting with an input boundary layer profile of 31 points in the normal coordinate at the same axial station. The experimental results [14] are also shown for comparison. Figure 5 shows that the calculated C_f agrees well with experiment for $0.6 < x_0 < 0.8$, but disagrees sharply both fore and aft of this interval. From Figure 6 one can see that the calculated θ is lower than experiment for the interval $0.6 < x_0 < 0.9$, but slightly higher aft of this interval. The calculated shape factor H in Figure 7 has very poor agreement with experiment. The reason for these disagreements is

attributed to the inability of the algebraic turbulence model to accurately simulate the large trip wire used in the experiment, and to the general inadequacy of the turbulence model in the tail region.

All these figures show that agreement between second- and fourth-order calculations is quite good; the differences between the two being indistinguishable on most of the body.

Boundary Layer Profiles

Figures 8-10 show the boundary layer profiles at axial coordinates of 0.601, 0.880, and 0.990, respectively. The calculated profile at $x_0 = 0.601$ (see Figure 8) reflects the influence of the large trip wire used in the experimental calculations; the calculated results near the wall are less full than the experimental results. At the two downstream stations where the effect of the large trip wire has died out, the opposite is true; the profiles are slightly too full near the wall, as can be seen in Figures 9 and 10, for $x_0 = 0.880$ and 0.990 respectively. These discrepancies are attributed to the inadequacy of the algebraic turbulence model near the tail of the body.

In Figures 8-10 the second- and fourth-order calculations are seen to be indistinguishable. Note that the fourth-order calculations were made with a mesh-spacing three times as large as that of the second-order calculations.

Computer Run Times

As mentioned previously, both the second- and fourth-order calculations were performed on the Penn State IBM 370/3033 computer system. The net C.P.U. time for the second-order calculations shown in the figures was

38 seconds, whereas the net C.P.U. time for the fourth-order calculations with one-third of the number of points in the input profile was 28 seconds. This represents a 26 percent decrease in run time for the fourth-order method.

CONCLUDING REMARKS

A fourth-order box solution of the incompressible, axisymmetric, laminar or turbulent boundary layer equations has been presented and, as an example, applied to a low-drag body of revolution. For this case, the fourth-order solution had an input mesh-spacing three times larger than that of a second-order solution, but provided results of equivalent accuracy and with 26 percent less computer run time. Fourth-order box solutions of other equations have also been found to provide the equivalent accuracy of second-order solutions with fewer mesh points and requiring less computer time. For example, Wornom [3] has achieved such a result for the two-dimensional stagnation point solution.

One disadvantage of the fourth-order box solution presented here should be noted. The solution sometimes has greater convergence difficulties at the outer edge of the boundary layer than does the second-order solution with the same input conditions. Convergence problems have been noted for solutions with very small mesh-spacing or with smaller convergence tolerances. These problems were especially prevalent when the one piece turbulence model of Glowacki [12] was tried. No convergence problems were encountered with the second-order method using this model, but the fourth-order method would not converge to a

solution aft of axial coordinate $x_0 = 0.880$. The reason for this behavior is not known; one possibility is that because of the increased complexity of the fourth-order coefficients, numerical noise is amplified as these coefficients get very small at the outer edge of the boundary layer. This problem requires further investigation .

Other fourth-order accurate methods are available which have not been considered in this paper. See, for example, a comparison of higher-order solutions by Rubin and Khosla [13]. On the other hand, spline methods may provide the same advantages as the fourth-order Keller box method, but with much less algebraic manipulation (a quantity of great abundance in the method presented in this paper).

References

1. Cebeci, T., and A. M. O. Smith, Analysis of Turbulent Boundary Layers, (Academic Press, New York, 1974).
2. Keller, H. B., "Some Computational Problems in Boundary Layer Flow," in Lecture Notes in Physics, Vol 35, (Springer-Verlag, Berlin, 1975), pp. 1 - 21.
3. Wornom, S. F., "A Fourth-Order Box Method for Solving the Boundary Layer Equations," NASA TM X-74000, 1977.
4. Cebeci, T., "Eddy-Viscosity Distribution in Thick Axisymmetric Boundary Layers," J. Fluids Eng., 95, 319, (1973).
5. Crawford, M. E., and W. M. Kays, "STAN5 - A Program for Numerical Computation of Two-Dimensional Internal and External Boundary Layer Flows," NASA CR-2742, December 1976.
6. Hoffman, G. H., Private Communications, 1978.
7. Clauser, F. H., "The Turbulent Boundary Layer," Advan. Appl. Mech., 4, 1, (1956).
8. Cebeci, T., "Kinematic Eddy Viscosity at Low Reynolds Numbers," AIAA J., 11, 102, (1973).
9. Chen, K. K., and N. A. Thyson, "Extension of Emmon's Spot Theory to Flows on Blunt Bodies," AIAA J., 9, 821, (1971).
10. Keller, H. B., "Accurate Difference Methods for Nonlinear Two-Point Boundary Value Problems," SIAM J. Numer. Anal., 11, 305, (1974).
11. Hoffman, G. H., "A Method for Calculating the Flow Field in the Tail Region of a Body of Revolution," ARL Technical Memorandum No. 78-211, 19 July 1978.
12. Glowacki, W. J., "An Improved Mixing Length Formulation for Turbulent Boundary Layers with Freestream Pressure Gradients," AIAA Paper 78-202, AIAA 16th Aerospace Sciences Meeting, Huntsville, Alabama, January 16-18, 1978.
13. Rubin, S. G., and P. K. Khosla, "Higher-Order Numerical Methods Derived from Three-Point Polynomial Interpolation," NASA CR-2735, August 1976.
14. Patel, V. C., and Y. T. Lee, "Thick Axisymmetric Turbulent Boundary Layer and Near Wake of a Low-Drag Body of Revolution," Iowa Institute of Hydraulic Research Report No. 210, December 1977.

Appendix A

Algebraic Eddy Viscosity Model

This appendix describes the details of the algebraic eddy viscosity model and treatment of the transition region. In this model the boundary layer is divided into an inner (law of the wall) and an outer (law of the wake) region; each region has its own equation with the junction between the two occurring when $\epsilon_1 = \epsilon_0$.

Inner Region

The inner eddy viscosity used is that of Crawford and Kays [5] as modified by Hoffman [6] for a thick axisymmetric boundary layer. The final form is

$$\epsilon_1 = \text{Re}^{3/2} \ell^2 \frac{r}{r_0} \left| \frac{\partial u}{\partial y} \right|, \quad (\text{A.1})$$

where ℓ is the mixing length given by

$$\ell = 0.41 Y \left[1 - \exp \left(-\frac{Y}{A} \right) \right], \quad (\text{A.2})$$

and Y is the modification for thick axisymmetric boundary layers mentioned above and is defined as

$$Y = \frac{r_0}{\cos \phi} \ln \frac{r}{r_0}. \quad (\text{A.3})$$

A is the sublayer thickness parameter; in universal (law of the wall) variables,

$$A^+ = A \text{Re } u_\tau, \quad (\text{A.4})$$

where u_τ is the dimensionless friction velocity given by

$$u_\tau = \left(\frac{1}{2} C_{f_\infty} \right)^{1/2}, \quad (\text{A.5})$$

and C_{f_∞} is the skin friction coefficient based on U_∞^* . The empirical formula of Crawford and Kays [5] is used for the sublayer thickness parameter, which for an impervious wall is

$$A^+ = \frac{A_{fp}^+}{1.0 + aP^+}, \quad (A.6)$$

where A_{fp}^+ is the flat plate value of $A^+ = 26.0$,

$$a = \begin{cases} 30.175 & \text{if } P^+ \leq 0 \\ 20.590 & \text{if } P^+ > 0 \end{cases}, \quad (A.7)$$

and
$$P^+ = \frac{u_e}{Re u_\tau} \frac{du_e}{dx}. \quad (A.8)$$

The above expression for A^+ was derived from data for equilibrium two-dimensional boundary layers. In a rapidly changing pressure gradient the boundary layer does not instantaneously adjust to a new equilibrium state. Instead, it tends to lag in its adjustment; to allow for this lag Crawford and Kays [5] have introduced a lag equation given by

$$\frac{dP_{eff}^+}{dx} = \frac{P^+ - P_{eff}^+}{T}, \quad (A.9)$$

where T is a time constant, P_{eff}^+ is the effective value of P^+ to be used in the relation for A^+ (Equation A.6), and P^+ is the local value of P^+ as given by Equation (A.8). The value of T used is Hoffman's modification [6] of Crawford and Kay's suggestion [5] which is

$$T = \frac{4000}{Re u_\tau}. \quad (A.10)$$

Equation (22) is solved by using centered differences and defining

$$\hat{P}^+ = \frac{P^+}{T}, \quad (A.11)$$

to get the finite-difference form

$$P_{eff,i+1}^+ = \frac{1}{\left(1 + \frac{\Delta x_i}{2T_{i+1}}\right)} \left[\left(1 - \frac{\Delta x_i}{2T_i}\right) P_{eff,i}^+ + \Delta x_i \hat{P}_{i+1/2}^+ \right]. \quad (A.12)$$

Equation (A.12) is an iterative equation because of the term T_{i+1} , so that each time the vector of unknowns at $(i+1)$ is updated in solving the non-linear finite-difference equations of motion, Equation (A.12) must also be updated.

Outer Region

In the outer region of the boundary layer the eddy viscosity is taken to be constant using the form suggested by Clauser which when non-dimensionalized becomes [7]

$$\epsilon_o = Re \alpha u_e \delta_k^* \quad , \quad (A.13)$$

where δ_k^* is the kinematic displacement thickness given by

$$\delta_k^* = \frac{1}{\sqrt{Re}} \int_0^\infty \left(1 - \frac{u}{u_e} \right) d\bar{y} \quad , \quad (A.14)$$

and α is a dimensionless quantity which accounts for low Reynolds number effects. Cebici has obtained the following expression for α [8]:

$$\alpha = \alpha_o \frac{1 + \pi_o}{1 + \pi} \quad (A.15)$$

where

$$\alpha_o = 0.0168 \quad , \quad (A.16)$$

$$\pi_o = 0.55 \quad , \quad (A.17)$$

$$\pi = \pi_o [1 - \exp(-0.243 \sqrt{Z} - 0.298 Z_1)] \quad , \quad (A.18)$$

$$Z_1 = \frac{Re_{\theta_k}}{425} - 1 \quad , \quad (A.19)$$

and Re_{θ_k} is the kinematic momentum thickness Reynolds number defined by

$$Re_{\theta_k} = Re \theta_k u_e \quad , \quad (A.20)$$

where

$$\theta_k = \frac{1}{\sqrt{Re}} \int_0^\infty \frac{u}{u_e} \left(1 - \frac{u}{u_e} \right) d\bar{y} \quad . \quad (A.21)$$

Note that when $Re_{\theta_k} < 425$, the argument of π in Equation (A.18) becomes imaginary. For this case one sets π to zero.

Transition Region

Since an algebraic eddy viscosity is used to model turbulence effects in the boundary layer, there is no built-in transition region. From an empirical curve fit discussed in Reference 6 a point is picked along the body where turbulence is "switched on," or tripped. It is not realistic to model the transition region by simply preceding from laminar to turbulent flow in one streamwise step. Therefore to account for the finite distance required in the transition region for the boundary layer to become fully turbulent, an intermittency factor γ_{tr} is used to reduce the intensity of the turbulence parameters. This factor, from Chen and Thyson [9], is given by

$$\gamma_{tr} = 1 - \exp(-g u_e^3 I_1 I_2) \quad , \quad (A.22)$$

where

$$g = \frac{Re^2}{1200} Re_{x_{tr}}^{-1.34} r_o(x_{tr}) \quad , \quad (A.23)$$

$$I_1 = \int_{x_{tr}}^x \frac{dx}{r_o} \quad , \quad (A.24)$$

$$I_2 = \int_{x_{tr}}^x \frac{dx}{u_e} \quad , \quad (A.25)$$

$$Re_{x_{tr}} = Re u_e x_{tr} \quad . \quad (A.26)$$

The trapezoidal rule is used in the computer code to evaluate the running integrals I_1 and I_2 . The eddy viscosities in the transition region are then multiplied by γ_{tr} to give

$$(\epsilon_1)_{tr} = \epsilon_1 \gamma_{tr} \quad , \quad (A.27)$$

$$(\epsilon_o)_{tr} = \epsilon_o \gamma_{tr} \quad . \quad (A.28)$$

Appendix B

Differentiation of Vector \vec{g}'

This appendix describes in detail the differentiation of the vector \vec{g}' with respect to \bar{y} to find \vec{g}'' in both the inner and outer regions of the boundary layer.

Inner Region

Equation (27) can be written in component form as

$$g_1' = -\frac{\partial \psi}{\partial x} \tau + \frac{r}{2} \frac{\partial}{\partial x} (u^2 - u_e^2) \quad , \quad (B.1)$$

$$g_2' = ru \quad , \quad (B.2)$$

$$g_3' = \tau \quad . \quad (B.3)$$

Differentiating Equation (B.1) yields

$$g_1'' = -\left(\frac{\partial \psi}{\partial x}\right)' \tau - \frac{\partial \psi}{\partial x} \tau' + \frac{1}{2} r' \frac{\partial}{\partial x} (u^2 - u_e^2) + \frac{r}{2} \left[\frac{\partial}{\partial x} (u^2 - u_e^2)\right]' \quad (B.4)$$

Using Equations (20)-(21) simplifies the above equation to

$$g_1'' = -\tau \frac{\partial}{\partial x} (ru) + (ru) \frac{\partial \tau}{\partial x} + \frac{\alpha}{2} \frac{\partial}{\partial x} (u^2 - u_e^2) - \frac{\partial \psi}{\partial x} \tau' \quad , \quad (B.5)$$

where from Equation (13),

$$\alpha = r' = \frac{\cos \phi}{\sqrt{Re}} \quad . \quad (B.6)$$

The second component of \vec{g}'' becomes

$$g_2'' = \alpha u + r\tau \quad , \quad (B.7)$$

and the third component becomes

$$g_3'' = \tau' \quad . \quad (B.8)$$

To evaluate τ' the product rule is applied to Equation (19) to get

$$rb\tau' + r\tau b' + ab\tau = \frac{r}{2} \frac{\partial}{\partial x} (u^2 - u_e^2) - \frac{\partial \psi}{\partial x} \tau \quad . \quad (B.9)$$

Differentiating Equation (18) and substituting Equation (28) yields

$$b' = s'\tau + s\tau' \quad , \quad (B.10)$$

where

$$s = C_e \tau / |\tau| \quad (B.11)$$

Thus, by substituting Equation (B.10) into (B.9) and isolating τ' , the following expression is obtained:

$$g_3'' = \tau' = \frac{1}{(1+2s\tau)} \left[\frac{1}{2} \frac{\partial}{\partial x} (u^2 - u_e^2) - \frac{\tau}{r} \frac{\partial \psi}{\partial x} - s'\tau^2 - \frac{\alpha}{r} \tau - \frac{\alpha}{r} s\tau^2 \right] \quad (B.12)$$

The value of τ obtained above must be substituted into Equation (B.5) to give

$$g_1'' = -\tau \frac{\partial}{\partial x} (ru) + (ru) \frac{\partial \tau}{\partial x} + \frac{\alpha}{2} \frac{\partial}{\partial x} (u^2 - u_e^2) - \frac{\partial \psi}{\partial x} \left(\frac{1}{1+2s\tau} \right) \left[\frac{1}{2} \frac{\partial}{\partial x} (u^2 - u_e^2) - \frac{\tau}{r} \frac{\partial \psi}{\partial x} - s'\tau^2 - \frac{\alpha}{r} \tau - \frac{\alpha}{r} s\tau^2 \right] \quad (B.13)$$

Combination of Equations (B.13), (B.7), and (B.12) yields the final form of \vec{g}''_{inner} as given by Equation (30).

Outer Region

In the differentiation of \vec{g}' in the outer region it becomes apparent that Equations (B.5) and (B.7) still hold. A different expression for τ' must be developed however because the eddy viscosity in the outer region is now a constant. From Equation (18) it is seen that b is also a constant; Equation (19) then becomes

$$rb\tau' + \alpha b\tau = \frac{r}{2} \frac{\partial}{\partial x} (u^2 - u_e^2) - \tau \frac{\partial \psi}{\partial x} \quad ,$$

which leads to

$$g_3'' = \tau' = \frac{1}{rb} \left[\frac{r}{2} \frac{\partial}{\partial x} (u^2 - u_e^2) - \alpha b\tau - \tau \frac{\partial \psi}{\partial x} \right] \quad (B.14)$$

Substitution of Equation (B.14) into (B.5) results in the following expression:

$$g_1'' = -\tau \frac{\partial}{\partial x} (ru) + (ru) \frac{\partial \tau}{\partial x} + \frac{\alpha}{2} \frac{\partial}{\partial x} (u^2 - u_e^2) - \frac{\partial \psi}{\partial x} \left(\frac{1}{rb} \right) \left[\frac{r}{2} \frac{\partial}{\partial x} (u^2 - u_e^2) - \alpha b\tau - \tau \frac{\partial \psi}{\partial x} \right] \quad (B.15)$$

Combination of Equations (B.15), (B.7) and (B.14) yields the final form of \vec{g}''_{outer} as given by Equation (31).

Appendix C

Derivation of Finite-Difference Expressions

This appendix describes in detail the derivation of the three linear finite-difference expressions given by Equations (32)-(34).

The first step in the derivation is to substitute Equations (26), (27), and either (30) or (31) into Equation (24) to obtain a set of first-order, nonlinear finite-difference expressions for either the inner or outer regions of the boundary layer. The inner layer is considered first; these expressions become

$$\begin{aligned}
 & (r\tau)_{j+1} + (rst^2)_{j+1} - (r\tau)_j - (rst^2)_j - \frac{hj}{2} \left[-\tau_{j+1} \frac{\partial}{\partial x} (\psi_{j+1}) + \left(\frac{r}{2}\right)_{j+1} \right. \\
 & \left. \frac{\partial}{\partial x} (u_{j+1}^2 - u_e^2) - \tau_j \frac{\partial}{\partial x} (\psi_j) + \left(\frac{r}{2}\right)_j \frac{\partial}{\partial x} (u_j^2 - u_e^2) \right] + \frac{hj^2}{12} \left\{ -\tau_{j+1} \frac{\partial}{\partial x} \right. \\
 & (ru)_{j+1} + (ru)_{j+1} \frac{\partial}{\partial x} (\tau_{j+1}) + \frac{\alpha}{2} \frac{\partial}{\partial x} (u_{j+1}^2 - u_e^2) - \frac{\partial}{\partial x} (\psi_{j+1}) \left(\frac{1}{1+2st} \right)_{j+1} \\
 & \left[\frac{1}{2} \frac{\partial}{\partial x} (u_{j+1}^2 - u_e^2) - \left(\frac{r}{2}\right)_{j+1} \frac{\partial}{\partial x} (\psi_{j+1}) - (s'\tau^2)_{j+1} - \left(\frac{\alpha}{r}\tau\right)_{j+1} - \right. \\
 & \left. \left(\frac{\alpha}{r}st^2\right)_{j+1} \right] + \tau_j \frac{\partial}{\partial x} (ru)_j - (ru)_j \frac{\partial}{\partial x} (\tau_j) - \frac{\alpha}{2} \frac{\partial}{\partial x} (u_j^2 - u_e^2) + \\
 & \left. \frac{\partial}{\partial x} (\psi_j) \left(\frac{1}{1+2st} \right)_j \left[\frac{1}{2} \frac{\partial}{\partial x} (u_j^2 - u_e^2) - \left(\frac{r}{2}\right)_j \frac{\partial}{\partial x} (\psi_j) - (s'\tau^2)_j - \left(\frac{\alpha}{r}\tau\right)_j - \right. \right. \\
 & \left. \left. \left(\frac{\alpha}{r}st^2\right)_j \right] \right\} = 0, \quad (C.1)
 \end{aligned}$$

$$\begin{aligned}
 & \psi_{j+1} - \psi_j - \frac{hj}{2} \left[(ru)_{j+1} + (ru)_j \right] + \frac{hj^2}{12} \left[au_{j+1} + (r\tau)_{j+1} - \right. \\
 & \left. au_j - (r\tau)_j \right] = 0, \quad (C.2)
 \end{aligned}$$

and

$$u_{j+1} - u_j - \frac{hj}{2} (\tau_{j+1} + \tau_j) + \frac{hj^2}{12} \left\{ \left(\frac{1}{1+2s\tau} \right)_{j+1} \left[\frac{1}{2} \frac{\partial}{\partial x} (u_{j+1}^2 - u_e^2) - \left(\frac{\tau}{r} \right)_{j+1} \frac{\partial}{\partial x} (\psi_{j+1}) - (s'\tau^2)_{j+1} - \left(\frac{\alpha}{r} \tau \right)_{j+1} - \left(\frac{\alpha}{r} s\tau^2 \right)_{j+1} \right] - \left(\frac{1}{1+2s\tau} \right)_j \left[\frac{1}{2} \frac{\partial}{\partial x} (u_j^2 - u_e^2) - \left(\frac{\tau}{r} \right)_j \frac{\partial}{\partial x} (\psi_j) - (s'\tau^2)_j - \left(\frac{\alpha}{r} \tau \right)_j - \left(\frac{\alpha}{r} s\tau^2 \right)_j \right] \right\} = 0. \quad (C.3)$$

Consider Equation (C.2) first. Since there are no x-derivatives it can be evaluated at $(i+1, j+1/2)$ which corresponds to point Q in Figure 2. Equations (C.1) and (C.3), however, contain x-derivatives which are approximated to second order by using central differences, and the expression is evaluated at point P in Figure 2, $(i+1/2, j+1/2)$, the center of the box element. The resulting expressions are quite lengthy and will not be shown here. However, some examples of terms which appear in Equations (C.1) and (C.3) appear below:

$$\frac{\partial}{\partial x} (\psi_j) = \frac{1}{\Delta x_i} (\psi_{i+1,j} - \psi_{i,j}), \quad (C.4)$$

$$s'\tau^2_{i+1/2,j+1} = \frac{1}{2} \left[(s'\tau^2)_{i+1,j+1} + (s'\tau^2)_{i,j+1} \right]. \quad (C.5)$$

As stated previously, the boundary layer equations are parabolic, that is, there is no upstream influence so that the solution is obtained by marching downstream. Thus, only the values along the station $(i+1)$ are unknown. The above expressions are nonlinear and must be linearized in order to obtain a solution. Since Newton's method is used to solve the finite-difference equations, the expressions are linearized about known values at station i and the known boundary conditions at station $(i+1)$, viz.

$$\left. \begin{aligned} \psi_{i+1,1}^{(1)} &= 0, \\ \psi_{i+1,j}^{(1)} &= \psi_{i,j}, \quad 2 \leq j \leq N, \\ \psi_{i+1,N+1}^{(1)} &= \psi_{i,N+1}, \end{aligned} \right\} \quad (C.6)$$

$$\left. \begin{aligned} u_{i+1,1}^{(1)} &= 0 \\ u_{i+1,j}^{(1)} &= u_{i,j}, \quad 2 \leq j \leq N, \\ u_{i+1,N+1}^{(1)} &= u_{e_{i+1}} \end{aligned} \right\} \quad (C.7)$$

and

$$\left. \begin{aligned} \tau_{i+1,1}^{(1)} &= \tau_{i,j} \\ \tau_{i+1,j}^{(1)} &= \tau_{i,j}, \quad 2 \leq j \leq N, \\ \tau_{i+1,N+1}^{(1)} &= \tau_{i,N+1}, \end{aligned} \right\} \quad (C.8)$$

where $j = N+1$ represents the grid point at the outer edge of the boundary layer and the superscript denotes the iteration count. The higher-order iterates are then

$$\left. \begin{aligned} \psi_{i+1,j}^{(n+1)} &= \psi_{i+1,j}^{(n)} + \delta\psi_{i+1,j}^{(n)}, \\ u_{i+1,j}^{(n+1)} &= u_{i+1,j}^{(n)} + \delta u_{i+1,j}^{(n)}, \\ \tau_{i+1,j}^{(n+1)} &= \tau_{i+1,j}^{(n)} + \delta\tau_{i+1,j}^{(n)}, \end{aligned} \right\} \quad n = 1, 2, \dots \quad (C.9)$$

which are introduced into the finite-difference equations developed from Equations (C.1)-(C.3), with only linear terms in the corrections being retained in the result. After much algebra, which will not be shown here, a coupled linear system for the corrections $(\delta\psi_{i+1,j}^{(n)}, \delta u_{i+1,j}^{(n)}, \delta\tau_{i+1,j}^{(n)})$ is obtained for $1 \leq j \leq N+1$, which is represented by Equations (32)-(34). The superscript n is understood in these expressions, and the coefficients are given by

$$\hat{A}_{i+1,j} = -2, \quad (C.10)$$

$$\hat{B}_{i+1,j} = -h_j r_{i+1,j} - \frac{h_j^2}{6} (\alpha_{i+1}), \quad (C.11)$$

$$\hat{C}_{i+1,j} = -\frac{h_j^2}{6} r_{i+1,j}, \quad (C.12)$$

$$\hat{D}_{i+1,j} = 2, \quad (C.13)$$

$$\hat{E}_{i+1,j} = -h_j r_{i+1,j+1} + \frac{h_j^2}{6} (\alpha_{i+1}), \quad (C.14)$$

$$\hat{F}_{i+1,j} = \frac{h_j^2}{6} r_{i+1,j+1}, \quad (C.15)$$

$$\begin{aligned} \hat{S}_{i+1,j} = & -2\psi_{i+1,j+1} + 2\psi_{i+1,j} + h_j \left[(ru)_{i+1,j+1} + (ru)_{i+1,j} \right] \\ & - \frac{h_j^2}{6} \left[\alpha_{i+1} (u_{i+1,j+1} - u_{i+1,j}) + (r\tau)_{i+1,j+1} - (r\tau)_{i+1,j} \right], \end{aligned} \quad (C.16)$$

$$\begin{aligned} \hat{A}_{i+1,j} = & \frac{h_j}{\Delta x_i} (\tau_{i+1,j} + \tau_{i,j}) + \frac{h_j^2}{6} \left(\frac{1}{\Delta x_i} \right) \left[-(\omega n)_{i+1,j} (\tau_{i+1,j} + \tau_{i,j}) \right. \\ & \left. + (H\sigma)_{i+1,j} \right], \end{aligned} \quad (C.17)$$

$$\begin{aligned} \hat{B}_{i+1,j} = & -2h_j (\beta u)_{i+1,j} + \frac{h_j^2}{3} \left(\frac{1}{\Delta x_i} \right) \left[(\omega u)_{i+1,j} \left(\frac{1}{\Delta x_i} \right) - (u\Lambda_o)_{i+1,j} \right. \\ & \left. + \tau_{i,j} r_{i+1,j} \right], \end{aligned} \quad (C.18)$$

$$\begin{aligned} \hat{C}_{i+1,j} = & -2r_{i+1,j} - 4 (sr\tau)_{i+1,j} + \frac{h_j}{\Delta x_i} (\psi_{i+1,j} - \psi_{i,j}) + \frac{h_j^2}{6} \left(\frac{1}{\Delta x_i} \right) \\ & \left[-(\omega n)_{i+1,j} (\psi_{i+1,j} - \psi_{i,j}) - (\omega\lambda)_{i+1,j} + (z\sigma)_{i+1,j} - 2(ru)_{i,j} \right], \end{aligned} \quad (C.19)$$

$$\hat{D}_2^2_{i+1,j} = \frac{h_j}{\Delta x_1} (\tau_{i+1,j+1} + \tau_{i,j+1}) + \frac{h_j^2}{6} \left(\frac{1}{\Delta x_1} \right) \left[(\omega\eta)_{i+1,j+1} (\tau_{i+1,j+1} + \tau_{i,j+1}) - (H\sigma)_{i+1,j+1} \right], \quad (C.20)$$

$$\hat{E}_2^2_{i+1,j} = -2h_j (\beta u)_{i+1,j+1} + \frac{h_j^2}{3} \left(\frac{1}{\Delta x_1} \right) \left[-(\omega u)_{i+1,j+1} \left(\frac{1}{\Delta x_1} \right) + (u\lambda_0)_{i+1,j+1} - \tau_{i,j+1} \tau_{i+1,j+1} \right], \quad (C.21)$$

$$\hat{F}_2^2_{i+1,j} = 2\tau_{i+1,j+1} + 4(sr\tau)_{i+1,j+1} + \frac{h_j}{\Delta x_1} (\psi_{i+1,j+1} - \psi_{i,j+1}) + \frac{h_j^2}{6} \left(\frac{1}{\Delta x_1} \right) \left[(\omega\eta)_{i+1,j+1} (\psi_{i+1,j+1} - \psi_{i,j+1}) + (\omega\lambda)_{i+1,j+1} - (z\sigma)_{i+1,j+1} + 2(ru)_{i,j+1} \right], \quad (C.22)$$

$$\begin{aligned} \hat{S}_2^2_{i+1,j} = & 2 \left[- (rb\tau)_{i+1,j+1} + (rb\tau)_{i+1,j} \right] + h_j \left\{ - \left(\frac{1}{\Delta x_1} \right) \left[\tau_{i+1,j+1} (\psi_{i+1,j+1} - \psi_{i,j+1}) + \tau_{i,j+1} \psi_{i+1,j+1} \right] + \beta_{i+1,j+1} (u^2_{i+1,j+1} + \gamma_{i+1,j+1}) - \left(\frac{1}{\Delta x_1} \right) \right. \\ & \left[\tau_{i+1,j} (\psi_{i+1,j} - \psi_{i,j}) + \tau_{i,j} \psi_{i+1,j} \right] + \beta_{i+1,j} (u^2_{i+1,j} + \gamma_{i+1,j}) \left. \right\} \\ & - \frac{h_j^2}{6} \left(\frac{1}{\Delta x_1} \right) \left\{ - (\omega\sigma)_{i+1,j+1} + \Lambda_{o_{i+1}} (u^2_{i+1,j+1} + \gamma_{i+1,j+1}) - 2 \left[-\tau_{i+1,j+1} (ru)_{i,j+1} + \tau_{i,j+1} (ru)_{i+1,j+1} \right] + (\omega\sigma)_{i+1,j} - \Lambda_{o_{i+1}} (u^2_{i+1,j} + \gamma_{i+1,j}) \right. \\ & \left. + 2 \left[-\tau_{i+1,j} (ru)_{i,j} + \tau_{i,j} (ru)_{i+1,j} \right] \right\} - \widetilde{S}_{i,j}^2 \quad (C.23) \end{aligned}$$

$$\widetilde{S}_2^{i,j} = 2 \left[(rb\tau)_{i,j+1} - (rb\tau)_{i,j} \right] - \frac{h_j}{\Delta x_1} \left[(\tau\psi)_{i,j+1} + (\tau\psi)_{i,j} \right], \quad (C.24)$$

$$\hat{A}_3^{i+1,j} = \frac{h_j^2}{6} (H\eta)_{i+1,j} (\tau_{i+1,j} + \tau_{i,j}), \quad (C.25)$$

$$\hat{B}_3^{i+1,j} = -2 - \frac{h_j^2}{3} \left(\frac{1}{\Delta x_1} \right) (Hu)_{i+1,j}, \quad (C.26)$$

$$\hat{C}_3^{i+1,j} = -h_j + \frac{h_j^2}{2} \left\{ (sH^2\sigma)_{i+1,j} + H_{i+1,j} \left[\eta_{i+1,j} (\psi_{i+1,j} - \psi_{i,j}) + \lambda_{i+1,j} \right] \right\}, \quad (C.27)$$

$$\hat{D}_3^{i+1,j} = -\frac{h_j^2}{6} (H\eta)_{i+1,j+1} (\tau_{i+1,j+1} + \tau_{i,j+1}), \quad (C.28)$$

$$\hat{E}_3^{i+1,j} = 2 + \frac{h_j^2}{3} \left(\frac{1}{\Delta x_1} \right) (Hu)_{i+1,j+1}, \quad (C.29)$$

$$\begin{aligned} \hat{F}_3^{i+1,j} = -h_j - \frac{h_j^2}{6} \left\{ (sH^2\sigma)_{i+1,j+1} + H_{i+1,j+1} \left[\eta_{i+1,j+1} (\psi_{i+1,j+1} \right. \right. \\ \left. \left. - \psi_{i,j+1}) + \lambda_{i+1,j+1} \right] \right\}, \end{aligned} \quad (C.30)$$

$$\begin{aligned} \hat{S}_3^{i+1,j} = 2(-u_{i+1,j+1} + u_{i+1,j}) + h_j (\tau_{i+1,j+1} + \tau_{i+1,j}) - \frac{h_j^2}{6} \\ \left[(H\sigma)_{i+1,j+1} - (H\sigma)_{i+1,j} \right] + \widetilde{S}_3^{i,j}, \end{aligned} \quad (C.31)$$

$$\widetilde{S}_3^{i,j} = 2(-u_{i,j+1} + u_{i,j}) + h_j (\tau_{i,j+1} + \tau_{i,j}), \quad (C.32)$$

where the various parameters in the above equations are defined by

$$\lambda_{i+1,j} = \left(\frac{\alpha}{r} \right)_{i+1,j} (1+2\epsilon)_{i+1,j} + 2(s'\tau)_{i+1,j} , \quad (C.33)$$

$$\eta_{i+1,j} = \frac{1}{2\Delta x_i} \left[\left(\frac{1}{r} \right)_{i+1,j} + \left(\frac{1}{r} \right)_{i,j} \right] , \quad (C.34)$$

$$\gamma_{i+1,j} = u_{e,i}^2 - u_{e,i+1}^2 - u_{i,j}^2 , \quad (C.35)$$

$$\beta_{i+1,j} = \frac{1}{\Delta x_i} \left[\left(\frac{r}{2} \right)_{i+1,j} + \left(\frac{r}{2} \right)_{i,j} \right] , \quad (C.36)$$

$$\Lambda_{o,i+1} = \frac{1}{2} (\alpha_{i+1} + \alpha_i) , \quad (C.37)$$

$$H_{i+1,j} = 1/(b_{i,j} + \epsilon_{i+1,j}) , \quad (C.38)$$

$$\begin{aligned} \sigma_{i+1,j} = & \frac{1}{\Delta x_i} (u_{i+1,j}^2 + \gamma_{i+1,j}) - \eta_{i+1,j} (\tau_{i+1,j} + \tau_{i,j}) (\psi_{i+1,j} - \psi_{i,j}) \\ & - \tau_{i+1,j} \left[\left(\frac{\alpha}{b} \right)_{i+1,j} + (s'\tau)_{i+1,j} \right] - \tau_{i,j} \left[\left(\frac{\alpha}{b} \right)_{i,j} + (s'\tau)_{i,j} \right] , \end{aligned} \quad (C.39)$$

$$\omega_{i+1,j} = H_{i+1,j} (\psi_{i+1,j} - \psi_{i,j}) , \quad (C.40)$$

$$z_{i+1,j} = (H^2 S)_{i+1,j} (\psi_{i,j} - \psi_{i+1,j}) . \quad (C.41)$$

The outer region must be considered next. Substitution of Equations (26), (27), and (31) into Equation (24) yields the following set of first-order, nonlinear, finite-difference expressions for the outer layer:

$$\begin{aligned}
 & (rb\tau)_{j+1} - (rb\tau)_j - \frac{h_j}{2} \left[-\tau_{j+1} \frac{\partial}{\partial x} (\psi_{j+1}) + \frac{r_{j+1}}{2} \frac{\partial}{\partial x} (u_{j+1}^2 - u_e^2) \right. \\
 & \left. - \tau_j \frac{\partial}{\partial x} (\psi_j) + \frac{r_j}{2} \frac{\partial}{\partial x} (u_j^2 - u_e^2) \right] + \frac{h_j^2}{12} \left\{ -\tau_{j+1} \frac{\partial}{\partial x} (ru)_{j+1} + (ru)_{j+1} \right. \\
 & \frac{\partial}{\partial x} (\tau_{j+1}) + \frac{\alpha}{2} \frac{\partial}{\partial x} (u_{j+1}^2 - u_e^2) - \frac{1}{br_{j+1}} \frac{\partial}{\partial x} (\psi_{j+1}) \left[\frac{r_{j+1}}{2} \frac{\partial}{\partial x} (u_{j+1}^2 - u_e^2) - \right. \\
 & \left. ab\tau_{j+1} - \tau_{j+1} \frac{\partial}{\partial x} (\psi_{j+1}) + \tau_j \frac{\partial}{\partial x} (ru)_j - (ru)_j \frac{\partial}{\partial x} (\tau_j) - \frac{\alpha}{2} \frac{\partial}{\partial x} (u_j^2 - u_e^2) + \right. \\
 & \left. \left. \frac{1}{br_j} \frac{\partial}{\partial x} (\psi_j) \left[\frac{r_j}{2} \frac{\partial}{\partial x} (u_j^2 - u_e^2) - ab\tau_j - \tau_j \frac{\partial}{\partial x} (\psi_j) \right] \right\} = 0, \quad (C.42)
 \end{aligned}$$

$$\begin{aligned}
 & u_{j+1} - u_j - \frac{h_j}{2} (\tau_{j+1} + \tau_j) + \frac{h_j^2}{12} \left\{ \frac{1}{br_{j+1}} \left[\frac{r_{j+1}}{2} \frac{\partial}{\partial x} (u_{j+1}^2 - u_e^2) - ab\tau_{j+1} \right. \right. \\
 & \left. \left. - \tau_{j+1} \frac{\partial}{\partial x} (\psi_{j+1}) \right] - \frac{1}{br_j} \left[\frac{r_j}{2} \frac{\partial}{\partial x} (u_j^2 - u_e^2) - ab\tau_j - \tau_j \frac{\partial}{\partial x} (\psi_j) \right] \right\} = 0 \quad (C.43)
 \end{aligned}$$

Note that the middle equation in this set was left out as it is identical to Equation (C.2) for the inner layer. The same procedure is applied now to the above equation set for the outer region as was applied to the inner set of equations. That is, they are approximated in the center of the box using central differences and then are linearized using Equations (C.6)-(C.9). The final result is the coupled linear system for the corrections $(\delta\psi_{i+1}^{(n)}, \delta u_{i+1,j}^{(n)}, \delta\tau_{i+1,j}^{(n)})$ represented by Equations (32)-(34). The form is identical to that of the inner layer, but with some modifications to the coefficients as shown below:

$$\begin{aligned}
 \hat{A}_{i+1,j}^2 &= \frac{h_j}{\Delta x_1} (\tau_{i+1,j} + \tau_{i,j}) + \frac{h_j^2}{6} \left(\frac{1}{\Delta x_1} \right) \sigma_{o\ i+1,j} \left[-(\psi_{i+1,j} - \psi_{i,j}) \left(\frac{1}{\Delta x_1} \right) \right. \\
 & \left. (\tau_{i+1,j} + \tau_{i,j}) + \gamma_{o\ i+1,j} \right], \quad (C.44)
 \end{aligned}$$

$$\hat{B}_2^{(2)}_{i+1,j} = -2h_j (\beta u)_{i+1,j} + \frac{h_j^2}{3} \left(\frac{1}{\Delta x_1} \right) \left[\tau_{i,j} r_{i+1,j} - (u\Lambda_0)_{i+1,j} + \sigma_{0\ i+1,j} (\psi_{i+1,j} - \psi_{i,j}) (\beta u)_{i+1,j} \right], \quad (C.45)$$

$$\hat{C}_2^{(2)}_{i+1,j} = -2 (rb)_{i+1,j} + \frac{h_j}{\Delta x_1} (\psi_{i+1,j} - \psi_{i,j}) + \frac{h_j^2}{6} \left(\frac{1}{\Delta x_1} \right) \left\{ -2(ru)_{i,j} + \sigma_{0\ i+1,j} (\psi_{i+1,j} - \psi_{i,j}) \left[-(b\Lambda_0)_{i+1,j} - \frac{1}{\Delta x_1} (\psi_{i+1,j} - \psi_{i,j}) \right] \right\}, \quad (C.46)$$

$$\hat{D}_2^{(2)}_{i+1,j} = \frac{h_j}{\Delta x_1} (\tau_{i+1,j+1} + \tau_{i,j+1}) + \frac{h_j^2}{6} \left(\frac{1}{\Delta x_1} \right) \sigma_{0\ i+1,j+1} (\psi_{i+1,j+1} - \psi_{i,j+1}) \left(\frac{1}{\Delta x_1} \right) (\tau_{i+1,j+1} + \tau_{i,j+1}) - \gamma_{0\ i+1,j+1}, \quad (C.47)$$

$$\hat{E}_2^{(2)}_{i+1,j} = -2h_j (\beta u)_{i+1,j+1} + \frac{h_j^2}{3} \left(\frac{1}{\Delta x_1} \right) \left[-\tau_{i,j+1} r_{i+1,j+1} + (u\Lambda_0)_{i+1,j+1} - 2\sigma_{0\ i+1,j+1} (\psi_{i+1,j+1} - \psi_{i,j+1}) (\beta u)_{i+1,j+1} \right], \quad (C.48)$$

$$\hat{F}_2^{(2)}_{i+1,j} = 2(rb)_{i+1,j+1} + \frac{h_j}{\Delta x_1} (\psi_{i+1,j+1} - \psi_{i,j+1}) + \frac{h_j^2}{6} \left(\frac{1}{\Delta x_1} \right) \left\{ 2(ru)_{i,j+1} - \sigma_{0\ i+1,j+1} (\psi_{i+1,j+1} - \psi_{i,j+1}) \left[-(b\Lambda_0)_{i+1,j+1} - \frac{1}{\Delta x_1} (\psi_{i+1,j+1} - \psi_{i,j+1}) \right] \right\}, \quad (C.49)$$

$$\begin{aligned} \hat{S}_{i+1,j}^2 = & 2 \left[-(rb\tau)_{i+1,j+1} + (rb\tau)_{i+1,j} - (rb\tau)_{i,j+1} + (rb\tau)_{i,j} \right] + h_j \left[-\left(\frac{1}{\Delta x_i}\right) \right. \\ & \omega_{0 \ i+1,j+1} + \beta_{i+1,j+1} (u_{i+1,j+1}^2 + \gamma_{i+1,j+1}) - \left(\frac{1}{\Delta x_i}\right) \omega_{0 \ i+1,j} + \beta_{i+1,j} \\ & (u_{i+1,j}^2 + \gamma_{i+1,j}) \left. \right] - \frac{h_j^2}{6} \left(\frac{1}{\Delta x_i}\right) \left\{ -(\sigma_0 \gamma_0)_{i+1,j+1} (\psi_{i+1,j+1} - \psi_{i,j+1}) + \right. \\ & \Lambda_{0 \ i+1} (u_{i+1,j+1}^2 + \gamma_{i+1,j+1}) - 2 \left[-\tau_{i+1,j+1} (ru)_{i,j+1} + \tau_{i,j+1} (ru)_{i+1,j+1} \right] \\ & + (\sigma_0 \gamma_0)_{i+1,j} (\psi_{i+1,j} - \psi_{i,j}) - \Lambda_{0 \ i+1} (u_{i+1,j}^2 + \gamma_{i+1,j}) + 2 \left[-\tau_{i+1,j} \right. \\ & \left. (ru)_{i,j} + \tau_{i,j} (ru)_{i+1,j} \right] \left. \right\} , \end{aligned} \quad (C.50)$$

$$\hat{A}_{i+1,j}^3 = \frac{h_j^2}{6} \left(\frac{1}{\Delta x_i}\right) \sigma_{0 \ i+1,j} (\tau_{i+1,j} + \tau_{i,j}) \quad (C.51)$$

$$\hat{B}_{i+1,j}^3 = -2 - \frac{h_j^2}{3} (\sigma_0 \beta u)_{i+1,j} , \quad (C.52)$$

$$\hat{C}_{i+1,j}^3 = -h_j + \frac{h_j^2}{6} (\sigma_0 \ i+1,j) \left[(b\Lambda_0)_{i+1,j} + \left(\frac{1}{\Delta x_i}\right) (\psi_{i+1,j} - \psi_{i,j}) \right] , \quad (C.53)$$

$$\hat{D}_{i+1,j}^3 = -\frac{h_j^2}{6} \left(\frac{1}{\Delta x_i}\right) \sigma_{0 \ i+1,j+1} (\tau_{i+1,j+1} + \tau_{i,j+1}) , \quad (C.54)$$

$$\hat{E}_{i+1,j}^3 = 2 + \frac{h_j^2}{3} (\sigma_0 \beta u)_{i+1,j+1} , \quad (C.55)$$

$$\hat{F}_{i+1,j}^3 = -h_j - \frac{h_j^2}{6} (\sigma_0 \ i+1,j+1) \left[(b\Lambda_0)_{i+1,j+1} + \left(\frac{1}{\Delta x_i}\right) (\psi_{i+1,j+1} - \psi_{i,j+1}) \right] , \quad (C.56)$$

$$\begin{aligned} \hat{S}_{i+1,j} = & 2(-u_{i+1,j+1} + u_{i+1,j}) + h_j (\tau_{i+1,j+1} + \tau_{i+1,j}) - \frac{h_j^2}{6} \\ & \left[(\sigma_0 \gamma_0)_{i+1,j+1} - (\sigma_0 \gamma_0)_{i+1,j} \right] + \tilde{S}_{i,j}, \end{aligned} \quad (C.57)$$

where $\beta_{i+1,j}$, $\gamma_{i+1,j}$, $\Lambda_{0\ i+1}$, and $\tilde{S}_{i,j}$ are defined as before and

$$\omega_{0\ i+1,j} = (\tau_{i+1,j} + \tau_{i,j}) (\psi_{i+1,j} - \psi_{i,j}), \quad (C.58)$$

$$\sigma_{0\ i+1,j} = \frac{1}{2} \left[\left(\frac{1}{rb} \right)_{i+1,j} + \left(\frac{1}{rb} \right)_{i,j} \right],$$

$$\begin{aligned} \gamma_{0\ i+1,j} = & \beta_{i+1,j} (u_{i+1,j}^2 + \gamma_{i+1,j}) - \Lambda_{0\ i+1} \left[(b\tau)_{i+1,j} + (b\tau)_{i,j} \right] \\ & - \left(\frac{1}{\Delta x_i} \right) \omega_{0\ i+1,j}. \end{aligned} \quad (C.59)$$

The remaining coefficients are the same as those of the inner layer.

Appendix D

Block Tridiagonal Matrix Solution

This appendix describes in detail the solution of the block tridiagonal matrix equation given by Equation (50).

Since this equation is block tridiagonal, L-U factorization can be used to solve it. Following Hoffman [6],

$$A_t = LU ; L = [\beta_j, I, 0] , U = [o, \alpha_j, \gamma_j] \quad (D.1)$$

where I is the unity 3x3 matrix and β , α , and γ are 3x3 matrices. Equation (50) then can be expressed as the two systems

$$LY = R , \quad (D.2)$$

$$UZ = Y . \quad (D.3)$$

The L-U factorization requires that

$$\alpha_1 = A_1 \quad (D.4)$$

$$\alpha_j = A_j - \beta_j \gamma_{j-1} , \quad 2 \leq j \leq N+1 , \quad (D.5)$$

$$\beta_j \alpha_{j-1} = B_j , \quad 2 \leq j \leq N+1 , \quad (D.6)$$

$$\gamma_j = C_j , \quad 1 \leq j \leq N , \quad (D.7)$$

and

$$y_1 = R_1 , \quad (D.8)$$

$$y_j = R_j - \beta_j y_{j-1} , \quad 2 \leq j \leq N+1 , \quad (D.9)$$

$$\alpha_{N+1} z_{N+1} = y_{N+1} , \quad (D.10)$$

$$\alpha_j z_j = y_j - \gamma_j z_{j+1} , \quad N \geq j \geq 1 . \quad (D.11)$$

Because the matrices of Equations (42)-(46) are only 3x3, the linear systems (D.4)-(D.11) can be inverted beforehand. Thus it is not necessary to use a generalized matrix inversion routine. Equation (D.4) becomes

$$\alpha_1 = \begin{bmatrix} 1 & 0 & 0 \\ 0 & 1 & 0 \\ \hat{A3}_1 & \hat{B3}_1 & \hat{C3}_1 \end{bmatrix} \quad (D.12)$$

For $j \geq 2$ the bottom row of B is zero; thus, from Equation (D.6) the bottom row of β_j will also be zero. Then, from Equation (D.5)

$$\begin{bmatrix} \alpha_{11} & \alpha_{12} & \alpha_{13} \\ \alpha_{21} & \alpha_{22} & \alpha_{23} \\ \alpha_{31} & \alpha_{32} & \alpha_{33} \end{bmatrix}_j = \begin{bmatrix} \hat{D1}_{j-1} & \hat{E1}_{j-1} & \hat{F1}_{j-1} \\ \hat{D2}_{j-1} & \hat{E2}_{j-1} & \hat{F2}_{j-1} \\ \hat{A3}_j & \hat{B3}_j & \hat{C3}_j \end{bmatrix} - \begin{bmatrix} \beta_{11} & \beta_{12} & \beta_{13} \\ \beta_{21} & \beta_{22} & \beta_{23} \\ 0 & 0 & 0 \end{bmatrix}_j \begin{bmatrix} 0 & 0 & 0 \\ 0 & 0 & 0 \\ \hat{D3}_{j-1} & \hat{E3}_{j-1} & \hat{F3}_{j-1} \end{bmatrix},$$

which yields the relations

$$\left. \begin{aligned} (\alpha_{11})_j &= \hat{D1}_{j-1} - (\beta_{13})_j \hat{D3}_{j-1} , \\ (\alpha_{12})_j &= \hat{E1}_{j-1} - (\beta_{13})_j \hat{E3}_{j-1} , \\ (\alpha_{13})_j &= \hat{F1}_{j-1} - (\beta_{13})_j \hat{F3}_{j-1} , \\ (\alpha_{21})_j &= \hat{D2}_{j-1} - (\beta_{23})_j \hat{D3}_{j-1} , \\ (\alpha_{22})_j &= \hat{E2}_{j-1} - (\beta_{23})_j \hat{E3}_{j-1} , \\ (\alpha_{23})_j &= \hat{F2}_{j-1} - (\beta_{23})_j \hat{F3}_{j-1} , \\ (\alpha_{31})_j &= \hat{A3}_j , \\ (\alpha_{32})_j &= \hat{B3}_j , \\ (\alpha_{33})_j &= \hat{C3}_j . \end{aligned} \right\} \quad (D.13)$$

For $j=N+1$, Equation (D.5) becomes

$$\begin{bmatrix} \alpha_{11} & \alpha_{12} & \alpha_{13} \\ \alpha_{21} & \alpha_{22} & \alpha_{23} \\ \alpha_{31} & \alpha_{32} & \alpha_{33} \end{bmatrix}_{N+1} = \begin{bmatrix} \hat{D1}_N & \hat{E1}_N & \hat{F1}_N \\ \hat{D2}_N & \hat{E2}_N & \hat{F2}_N \\ 0 & 1 & 0 \end{bmatrix} - \begin{bmatrix} \beta_{11} & \beta_{12} & \beta_{13} \\ \beta_{21} & \beta_{22} & \beta_{23} \\ 0 & 0 & 0 \end{bmatrix}_{N+1} \begin{bmatrix} 0 & 0 & 0 \\ 0 & 0 & 0 \\ \hat{D3}_N & \hat{E3}_N & \hat{F3}_N \end{bmatrix}, \quad (D.14)$$

which yields

$$\alpha_{N+1} = \begin{bmatrix} \alpha_{11} & \alpha_{12} & \alpha_{13} \\ \alpha_{21} & \alpha_{22} & \alpha_{23} \\ 0 & 1 & 0 \end{bmatrix}_{N+1}, \quad (D.15)$$

where the first two rows are the same as Equations (D.13) with $j = N+1$ and $j-1=N$. Only the last row changes and is given by Equation (D.15).

Two cases must be considered for Equation (D.6), namely, $j=2$ and $2 \leq j \leq N$. For $j=2$,

$$\begin{bmatrix} \beta_{11} & \beta_{12} & \beta_{13} \\ \beta_{21} & \beta_{22} & \beta_{23} \\ 0 & 0 & 0 \end{bmatrix}_2 \begin{bmatrix} 1 & 0 & 0 \\ 0 & 1 & 0 \\ \hat{A3}_1 & \hat{B3}_1 & \hat{C3}_1 \end{bmatrix} = \begin{bmatrix} \hat{A1}_1 & \hat{B1}_1 & \hat{C1}_1 \\ \hat{A2}_1 & \hat{B2}_1 & \hat{C2}_1 \\ 0 & 0 & 0 \end{bmatrix}, \quad (D.16)$$

which yields the solutions

$$\left. \begin{aligned} (\beta_{11})_2 &= (\hat{A1}_1 \hat{C3}_1 - \hat{C1}_1 \hat{A3}_1) / \Delta_2, \\ (\beta_{12})_2 &= (\hat{B1}_1 \hat{C3}_1 - \hat{B3}_1 \hat{C1}_1) / \Delta_2, \\ (\beta_{13})_2 &= \hat{C1}_1 / \Delta_2, \\ (\beta_{21})_2 &= (\hat{A2}_1 \hat{C3}_1 - \hat{C2}_1 \hat{A3}_1) / \Delta_2, \\ (\beta_{22})_2 &= (\hat{B2}_1 \hat{C3}_1 - \hat{B3}_1 \hat{C2}_1) / \Delta_2, \\ (\beta_{23})_2 &= \hat{C2}_1 / \Delta_2, \end{aligned} \right\} \quad (D.17)$$

where

$$\Delta_2 = \hat{C}3_1 \quad . \quad (D.18)$$

For $j > 2$, Equation (D.6) becomes

$$\begin{bmatrix} \beta_{11} & \beta_{12} & \beta_{13} \\ \beta_{21} & \beta_{22} & \beta_{23} \\ 0 & 0 & 0 \end{bmatrix}_j \begin{bmatrix} \alpha_{11} & \alpha_{12} & \alpha_{13} \\ \alpha_{21} & \alpha_{22} & \alpha_{23} \\ \alpha_{31} & \alpha_{32} & \alpha_{33} \end{bmatrix}_{j-1} = \begin{bmatrix} \hat{A}1_{j-1} & \hat{B}1_{j-1} & \hat{C}1_{j-1} \\ \hat{A}2_{j-1} & \hat{B}2_{j-1} & \hat{C}2_{j-1} \\ 0 & 0 & 0 \end{bmatrix} \quad , \quad (D.19)$$

which gives

$$\begin{aligned} (\beta_{11})_j &= \left[(\hat{A}1 \alpha_{22} \alpha_{33})_{j-1} + (\hat{C}1 \alpha_{21} \alpha_{32})_{j-1} + (\hat{B}1 \alpha_{23} \alpha_{31})_{j-1} \right. \\ &\quad \left. - (\hat{C}1 \alpha_{22} \alpha_{31})_{j-1} - (\hat{A}1 \alpha_{23} \alpha_{32})_{j-1} - (\hat{B}1 \alpha_{21} \alpha_{33})_{j-1} \right] / \Delta_j , \\ (\beta_{12})_j &= \left[(\hat{B}1 \alpha_{11} \alpha_{33})_{j-1} + (\hat{A}1 \alpha_{32} \alpha_{13})_{j-1} + (\hat{C}1 \alpha_{31} \alpha_{12})_{j-1} \right. \\ &\quad \left. - (\hat{B}1 \alpha_{31} \alpha_{13})_{j-1} - (\hat{C}1 \alpha_{32} \alpha_{11})_{j-1} - (\hat{A}1 \alpha_{33} \alpha_{12})_{j-1} \right] / \Delta_j , \\ (\beta_{13})_j &= \left[(\hat{C}1 \alpha_{11} \alpha_{22})_{j-1} + (\hat{B}1 \alpha_{21} \alpha_{13})_{j-1} + (\hat{A}1 \alpha_{12} \alpha_{23})_{j-1} \right. \\ &\quad \left. - (\hat{A}1 \alpha_{22} \alpha_{13})_{j-1} - (\hat{B}1 \alpha_{11} \alpha_{23})_{j-1} - (\hat{C}1 \alpha_{12} \alpha_{21})_{j-1} \right] / \Delta_j , \\ (\beta_{21})_j &= \left[(\hat{A}2 \alpha_{22} \alpha_{33})_{j-1} + (\hat{C}2 \alpha_{21} \alpha_{32})_{j-1} + (\hat{B}2 \alpha_{23} \alpha_{31})_{j-1} \right. \\ &\quad \left. - (\hat{C}2 \alpha_{22} \alpha_{31})_{j-1} - (\hat{A}2 \alpha_{23} \alpha_{32})_{j-1} - (\hat{B}2 \alpha_{21} \alpha_{33})_{j-1} \right] / \Delta_j , \\ (\beta_{22})_j &= \left[(\hat{B}2 \alpha_{11} \alpha_{33})_{j-1} + (\hat{A}2 \alpha_{32} \alpha_{13})_{j-1} + (\hat{C}2 \alpha_{31} \alpha_{12})_{j-1} \right. \\ &\quad \left. - (\hat{B}2 \alpha_{31} \alpha_{13})_{j-1} - (\hat{C}2 \alpha_{32} \alpha_{11})_{j-1} - (\hat{A}2 \alpha_{33} \alpha_{12})_{j-1} \right] / \Delta_j , \\ (\beta_{23})_j &= \left[(\hat{C}2 \alpha_{11} \alpha_{22})_{j-1} + (\hat{B}2 \alpha_{21} \alpha_{13})_{j-1} + (\hat{A}2 \alpha_{12} \alpha_{23})_{j-1} \right. \\ &\quad \left. - (\hat{A}2 \alpha_{22} \alpha_{13})_{j-1} - (\hat{B}2 \alpha_{11} \alpha_{23})_{j-1} - (\hat{C}2 \alpha_{12} \alpha_{21})_{j-1} \right] / \Delta_j , \end{aligned} \quad (D.20)$$

where

$$\Delta_j = (\alpha_{11} \alpha_{22} \alpha_{33})_{j-1} + (\alpha_{21} \alpha_{32} \alpha_{13})_{j-1} + (\alpha_{31} \alpha_{12} \alpha_{23})_{j-1} \\ - (\alpha_{31} \alpha_{22} \alpha_{13})_{j-1} - (\alpha_{11} \alpha_{32} \alpha_{23})_{j-1} - (\alpha_{21} \alpha_{12} \alpha_{33})_{j-1} \quad (D.21)$$

Next, solve Equations (D.8) and (D.9) for y_j . Now

$$y_j = \begin{bmatrix} Y1 \\ Y2 \\ Y3 \end{bmatrix}_j \quad (D.22)$$

Hence, Equation (D.8) yields the three relations

$$\left. \begin{aligned} (Y1)_1 &= 0 \\ (Y2)_1 &= 0 \\ (Y3)_1 &= \hat{S3}_1 \end{aligned} \right\} \quad (D.23)$$

Equation (D.9) reads

$$\begin{bmatrix} Y1 \\ Y2 \\ Y3 \end{bmatrix}_j = \begin{bmatrix} \hat{S1}_{j-1} \\ \hat{S2}_{j-1} \\ \hat{S3}_j \end{bmatrix} - \begin{bmatrix} \beta_{11} & \beta_{12} & \beta_{12} \\ \beta_{21} & \beta_{22} & \beta_{23} \\ 0 & 0 & 0 \end{bmatrix}_j \begin{bmatrix} Y1 \\ Y2 \\ Y3 \end{bmatrix}_{j-1} \quad (D.24)$$

Upon expansion, for $2 \leq j \leq N+1$, the solutions are

$$\left. \begin{aligned} (Y1)_j &= \hat{S1}_{j-1} - (\beta_{11})_j (Y1)_{j-1} - (\beta_{12})_j (Y2)_{j-1} - (\beta_{13})_j (Y3)_{j-1} \\ (Y2)_j &= \hat{S2}_{j-1} - (\beta_{21})_j (Y1)_{j-1} - (\beta_{22})_j (Y2)_{j-1} - (\beta_{23})_j (Y3)_{j-1} \\ (Y3)_j &= \hat{S3}_j \end{aligned} \right\} \quad (D.25)$$

except that at $j=N+1$,

$$(Y3)_{N+1} = 0, \quad (D.26)$$

which follows from Equation (49). Now solve Equation (D.10) for Z_{N+1} using Equation (D.15):

$$\begin{bmatrix} \alpha_{11} & \alpha_{12} & \alpha_{13} \\ \alpha_{21} & \alpha_{22} & \alpha_{23} \\ 0 & 1 & 0 \end{bmatrix}_{N+1} \begin{bmatrix} \delta\psi \\ \delta u \\ \delta\tau \end{bmatrix}_{N+1} = \begin{bmatrix} Y1 \\ Y2 \\ 0 \end{bmatrix}_{N+1}, \quad (D.27)$$

which upon expansion and solving for the corrections yields

$$\left. \begin{aligned} (\delta\psi)_{N+1} &= \left[(\alpha_{13})_{N+1} (Y2)_{N+1} - (\alpha_{23})_{N+1} (Y1)_{N+1} \right] / \theta_{N+1}, \\ (\delta u)_{N+1} &= 0, \\ (\delta\tau)_{N+1} &= \left[(\alpha_{21})_{N+1} (Y1)_{N+1} - (\alpha_{11})_{N+1} (Y2)_{N+1} \right] / \theta_{N+1}, \end{aligned} \right\} \quad (D.28)$$

where

$$\theta_{N+1} = (\alpha_{13} \alpha_{21})_{N+1} - (\alpha_{11} \alpha_{23})_{N+1} \quad (D.29)$$

Next, solve for Z_j from Equation (D.11) for $2 \leq j \leq N$.

$$\begin{bmatrix} \alpha_{11} & \alpha_{12} & \alpha_{13} \\ \alpha_{21} & \alpha_{22} & \alpha_{23} \\ \alpha_{31} & \alpha_{32} & \alpha_{33} \end{bmatrix}_j \begin{bmatrix} \delta\psi \\ \delta u \\ \delta\tau \end{bmatrix}_j = \begin{bmatrix} Y1 \\ Y2 \\ Y3 \end{bmatrix}_j - \begin{bmatrix} 0 & 0 & 0 \\ 0 & 0 & 0 \\ \hat{D3}_j & \hat{E3}_j & \hat{F3}_j \end{bmatrix} \begin{bmatrix} \delta\psi \\ \delta u \\ \delta\tau \end{bmatrix}_{j+1}, \quad (D.30)$$

which yields the three equations for the correction vectors

$$\left. \begin{aligned} (\delta\psi)_j &= \left[(Y1 \alpha_{22} \alpha_{33})_j + (r3 \alpha_{12} \alpha_{23})_j + (Y2 \alpha_{13} \alpha_{32})_j \right. \\ &\quad \left. - (r3 \alpha_{22} \alpha_{13})_j - (Y1 \alpha_{23} \alpha_{32})_j - (Y2 \alpha_{12} \alpha_{33})_j \right] / \phi_j, \\ (\delta u)_j &= \left[(Y2 \alpha_{11} \alpha_{33})_j + (Y1 \alpha_{23} \alpha_{31})_j + (r3 \alpha_{13} \alpha_{21})_j \right. \\ &\quad \left. - (Y2 \alpha_{13} \alpha_{31})_j - (r3 \alpha_{11} \alpha_{23})_j - (Y1 \alpha_{21} \alpha_{33})_j \right] / \phi_j, \\ (\delta\tau)_j &= \left[(r3 \alpha_{11} \alpha_{22})_j + (Y2 \alpha_{12} \alpha_{31})_j + (Y1 \alpha_{21} \alpha_{32})_j \right. \\ &\quad \left. - (Y1 \alpha_{22} \alpha_{31})_j - (Y2 \alpha_{11} \alpha_{32})_j - (r3 \alpha_{12} \alpha_{21})_j \right] / \phi_j, \end{aligned} \right\} \quad (D.31)$$

where

$$r3_j = (Y3)_j - \hat{D3}_j (\delta\psi)_{j+1} - \hat{E3}_j (\delta u)_{j+1} - \hat{F3}_j (\delta\tau)_{j+1} , \quad (D.32)$$

and ϕ_j is identical to Δ_{j+1} as defined by Equation (D.21), or,

$$\begin{aligned} \phi_j &= (\alpha_{11} \alpha_{22} \alpha_{33})_j + (\alpha_{12} \alpha_{23} \alpha_{31})_j + (\alpha_{13} \alpha_{21} \alpha_{32})_j - (\alpha_{13} \alpha_{22} \alpha_{31})_j \\ &\quad - (\alpha_{11} \alpha_{23} \alpha_{32})_j - (\alpha_{12} \alpha_{21} \alpha_{33})_j = \Delta_{j+1} . \end{aligned} \quad (D.33)$$

Note; Equations (D.31) hold for $2 \leq j \leq N$. For $j=1$, use Equation (D.12) to get

$$\begin{bmatrix} 1 & 0 & 0 \\ 0 & 1 & 0 \\ \hat{A3}_1 & \hat{B3}_1 & \hat{C3}_1 \end{bmatrix} \begin{bmatrix} \delta\psi_1 \\ \delta u_1 \\ \delta\tau_1 \end{bmatrix} = \begin{bmatrix} 0 \\ 0 \\ \hat{Y3}_1 \end{bmatrix} \begin{bmatrix} 0 & 0 & 0 \\ 0 & 0 & 0 \\ \hat{D3}_1 & \hat{E3}_1 & \hat{F3}_1 \end{bmatrix} \begin{bmatrix} \delta\psi_2 \\ \delta u_2 \\ \delta\tau_2 \end{bmatrix} , \quad (D.34)$$

which yields the solutions

$$\left. \begin{aligned} \delta\psi_1 &= 0 , \\ \delta u_1 &= 0 , \\ \delta\tau_1 &= r3_1/\Delta_2 , \end{aligned} \right\} \quad (D.35)$$

where $r3$ is given by Equation (D.32) and Δ_2 by Equation (D.18).

February 2, 1979
JMC:cac

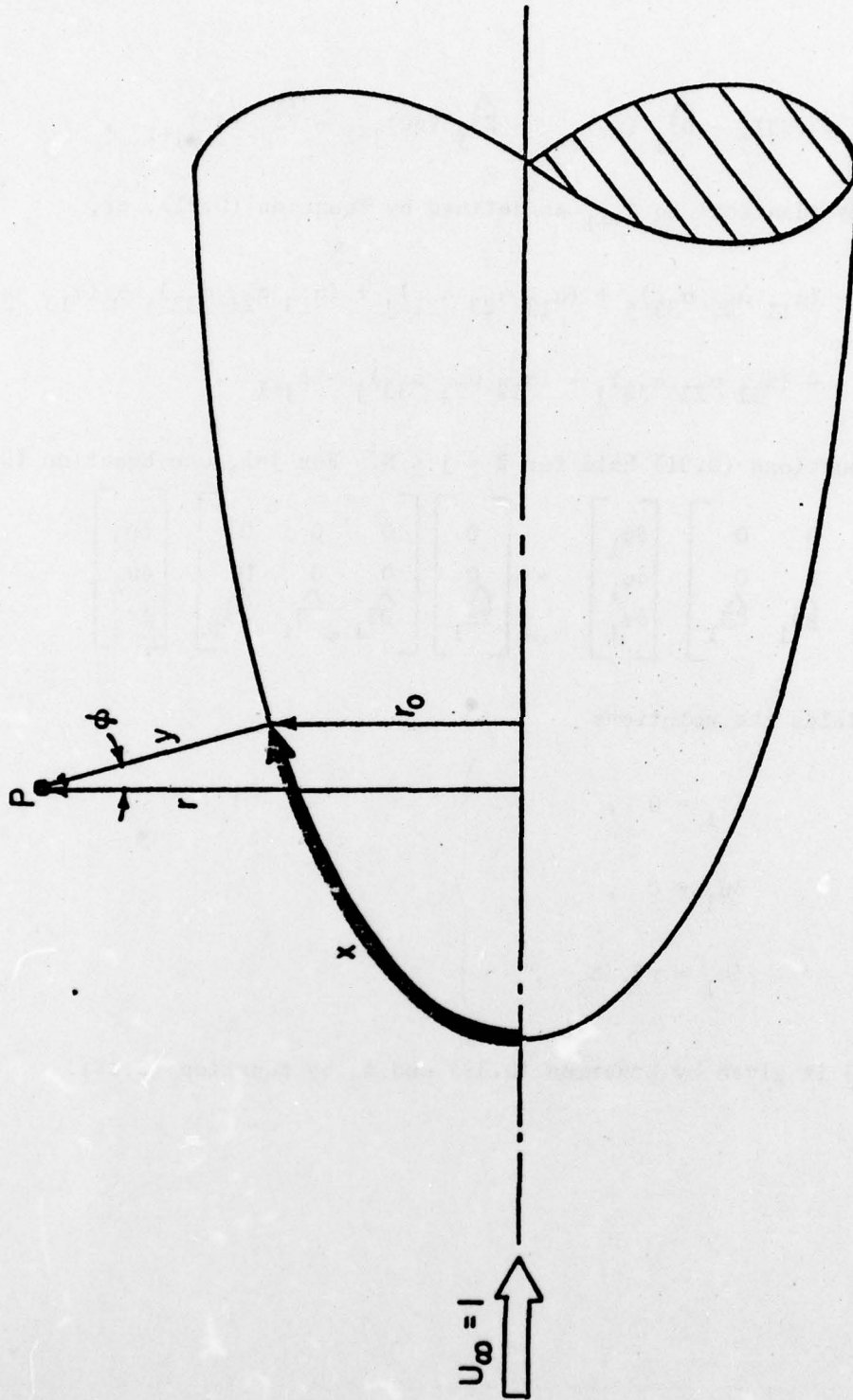


Figure 1 - Coordinate System for Body of Revolution

February 2, 1979
JMC:cac

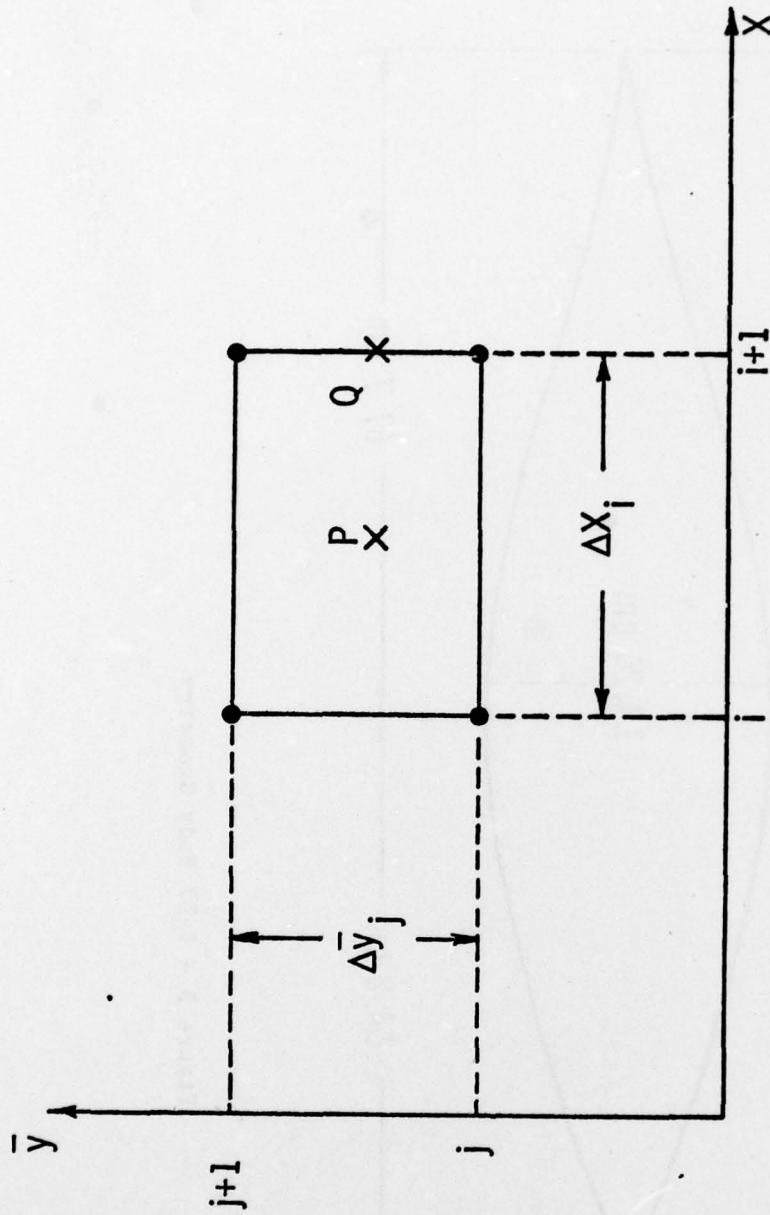


Figure 2 - Box Element for Finite Difference Approximation

February 2, 1979
JMC:cac

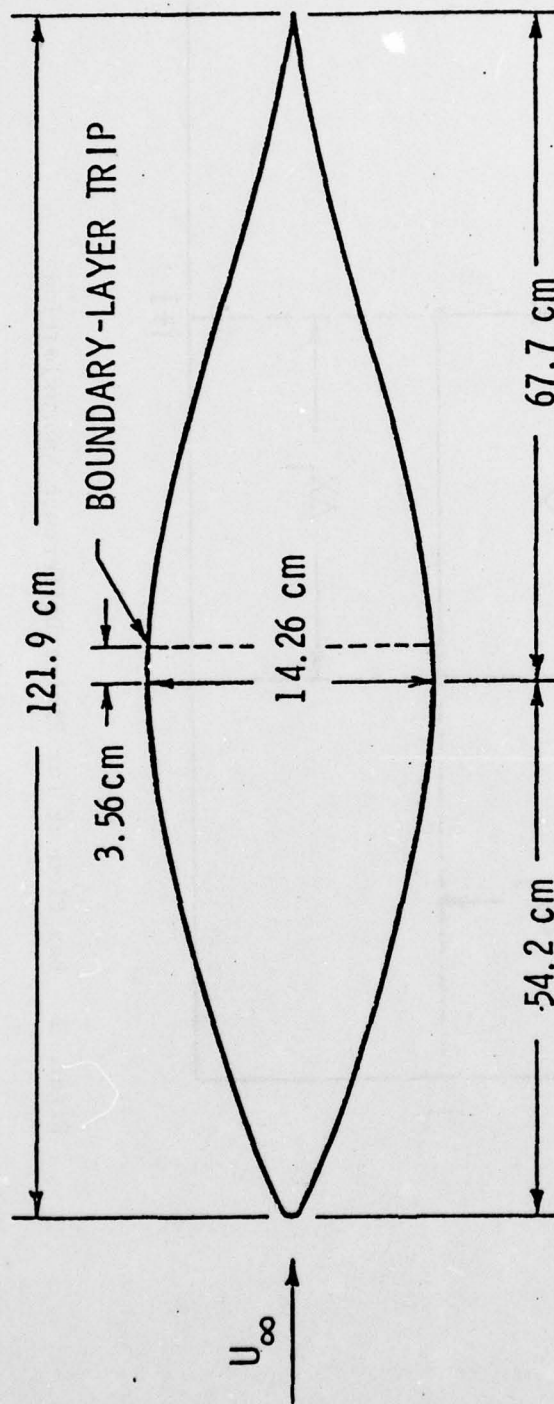


Figure 3 - F-57 Body Geometry

February 2, 1979
JMC:cac

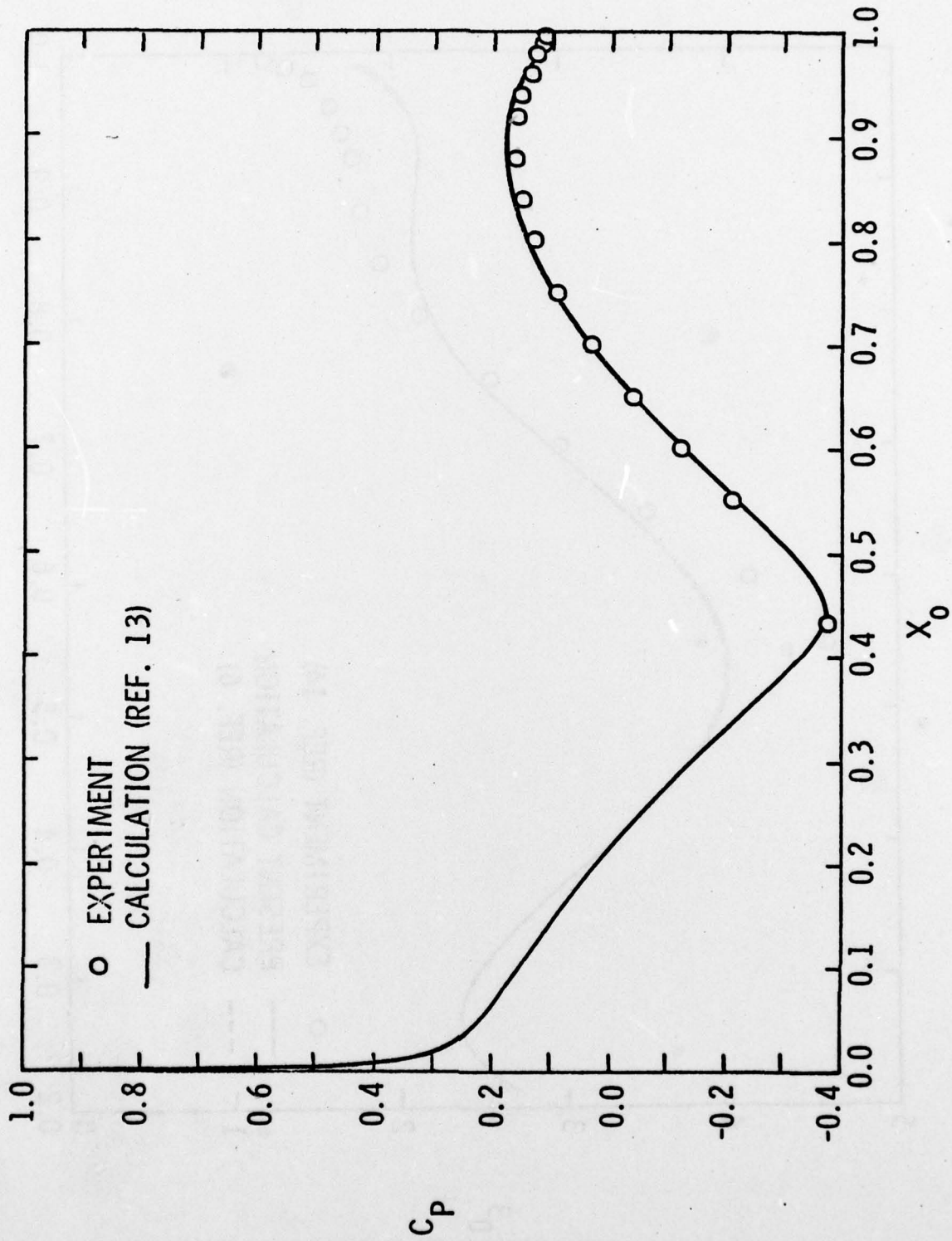


Figure 4 - Pressure Distribution, F-57 Body, $Re = 1.2 \times 10^6$

February 2, 1979
JMC:cac

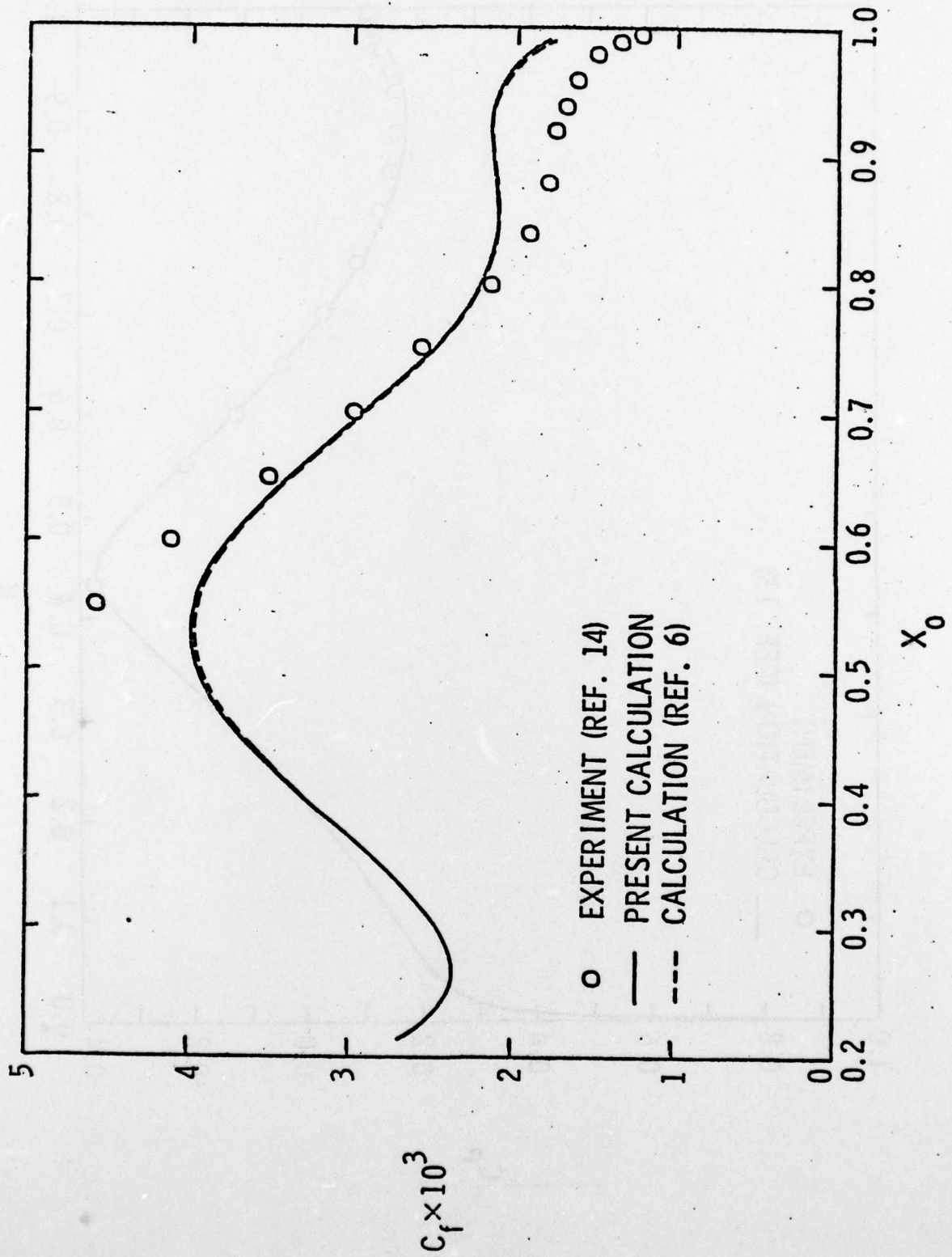


Figure 5 - Wall Friction Coefficient, F-57 Body, $Re = 1.2 \times 10^6$

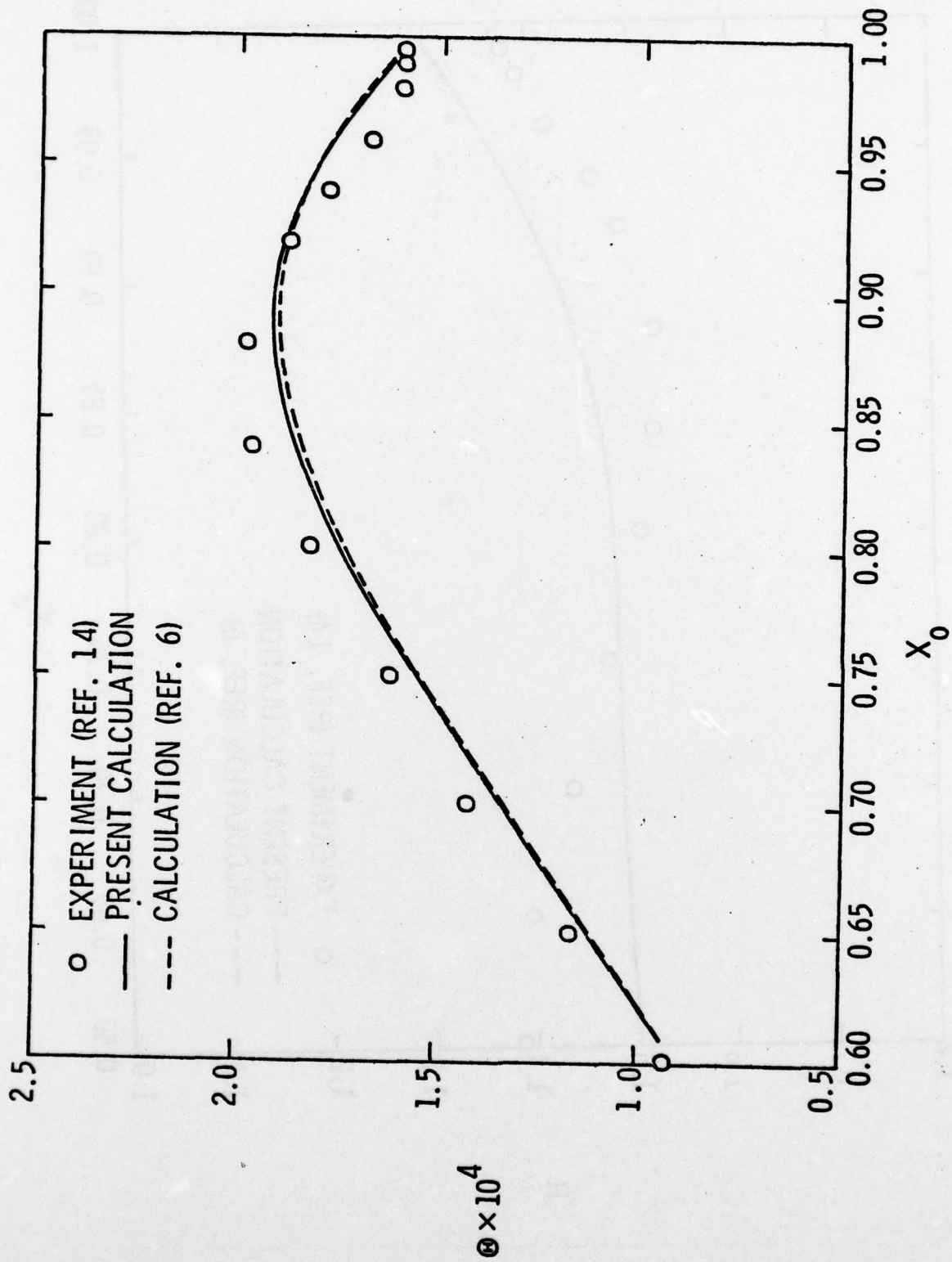


Figure 6 - Momentum Area Deficit, F-57 Body, $Re = 1.2 \times 10^6$

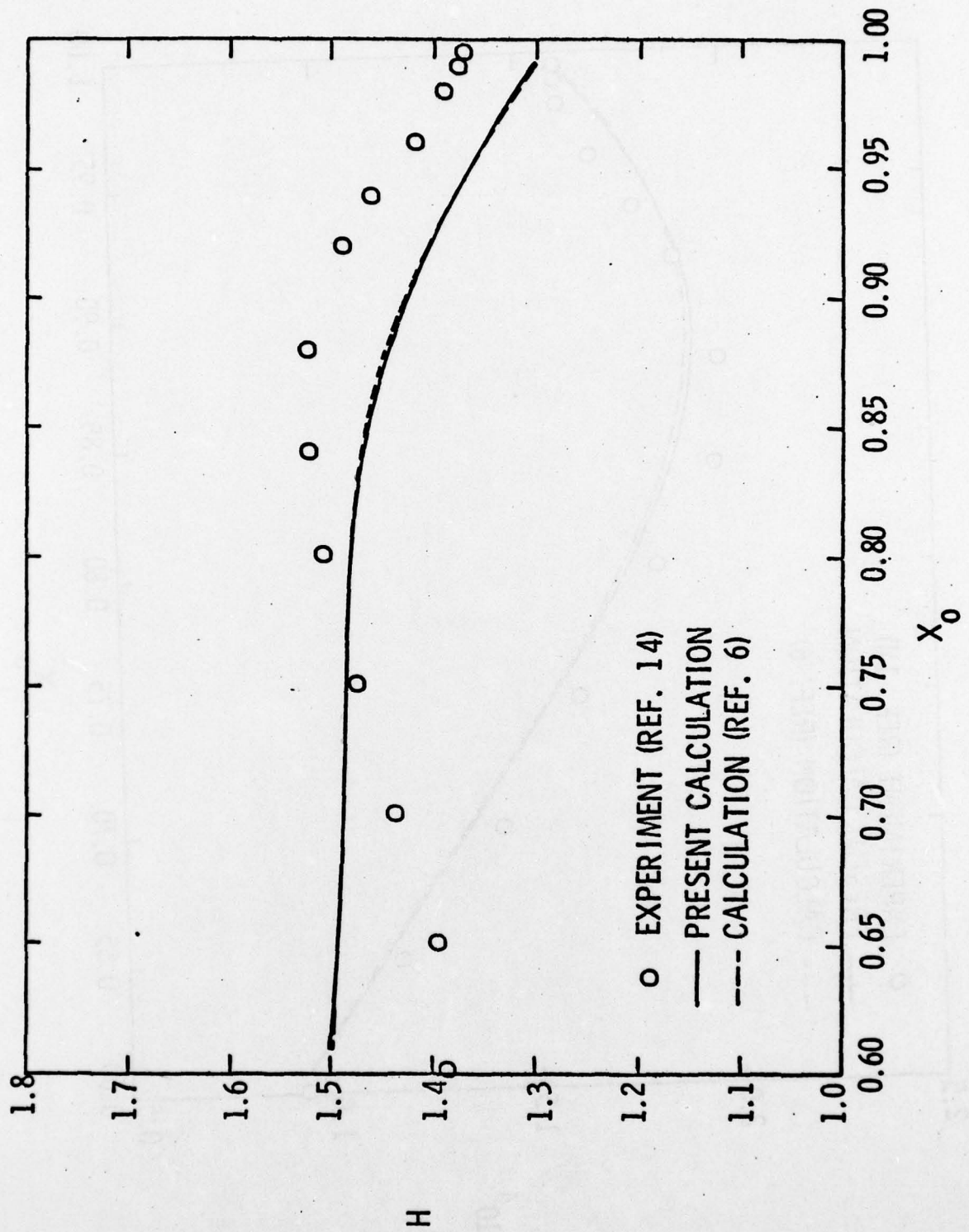


Figure 7 - Boundary Layer Shape Factor, F-57 Body, $Re = 1.2 \times 10^6$

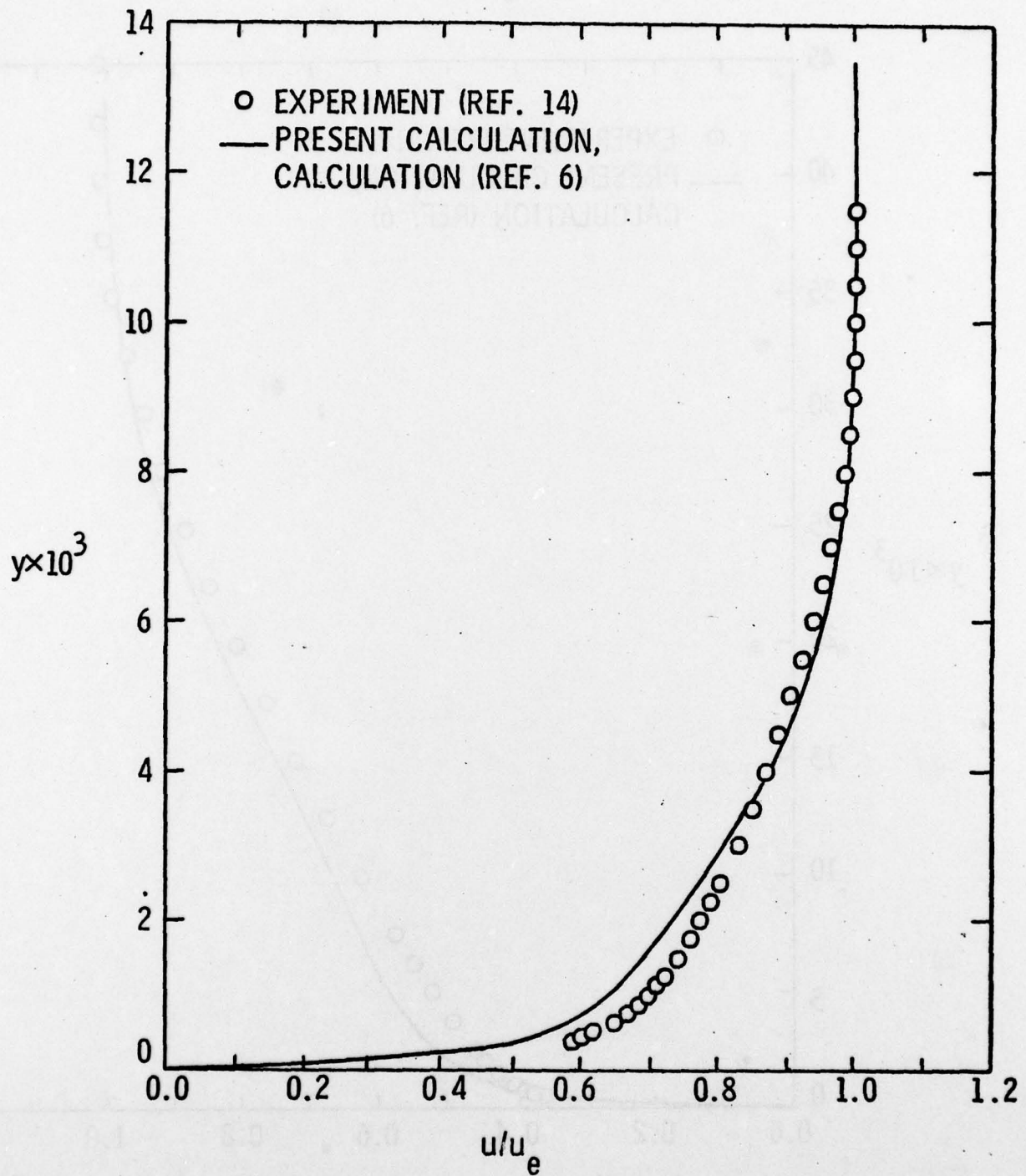


Figure 8 - Mean Velocity Profile at $X_0 = 0.601$, F-57 Body

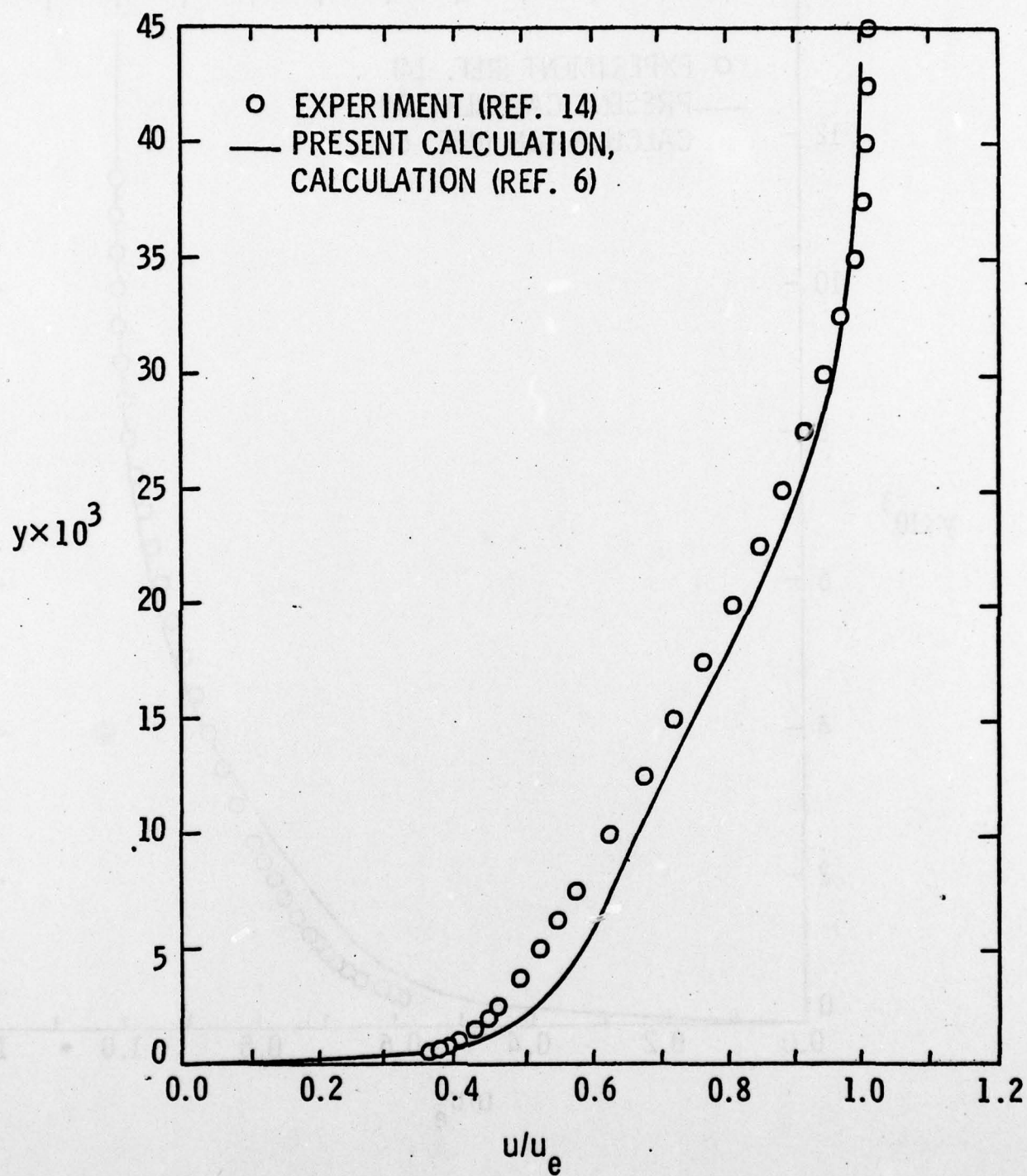


Figure 9 - Mean Velocity Profile at $X_0 = 0.880$, F-57 Body

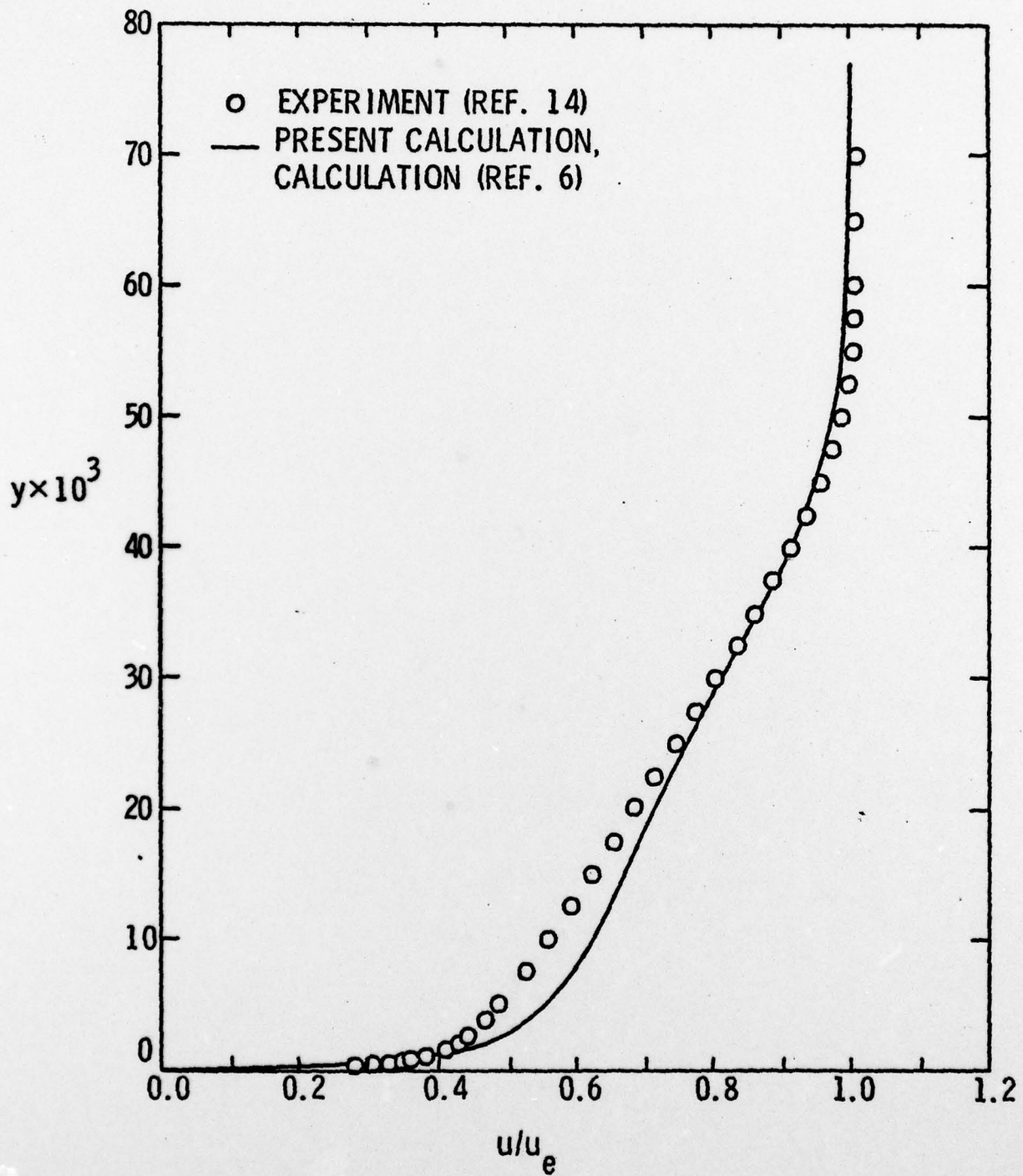


Figure 10 - Mean Velocity Profile at $X_0 = 0.990$, F-57 Body

DISTRIBUTION LIST FOR UNCLASSIFIED TM 79-18 by J. M. Cimbala, dated
February 2, 1979

Commander
Naval Sea Systems Command
Department of the Navy
Washington, DC 20362
Attn: Library
Code NSEA-09G32
(Copies No. 1 and 2)

Naval Sea Systems Command
Attn: C. G. McGuigan
Code NSEA-03133
(Copy No. 3)

Naval Sea Systems Command
Attn: E. G. Liszka
Code NSEA-0342
(Copy No. 4)

Naval Sea Systems Command
Attn: G. Sorkin
Code NSEA-035
(Copy No. 5)

Naval Sea Systems Command
Attn: T. E. Peirce
Code NSEA-0351
(Copy No. 6)

Naval Sea Systems Command
Attn: J. G. Juergens
Code NSEA-037
(Copy No. 7)

Naval Sea Systems Command
Attn: H. C. Claybourne
Code NSEA-0371
(Copy No. 8)

Naval Sea Systems Command
Attn: A. R. Paladino
Code NSEA-0372
(Copy No. 9)

Commander
Naval Ship Engineering Center
Department of the Navy
Washington DC 20362
Attn: F. Welling
Code NSEC-6144
(Copy No. 10)

Commanding Officer
Naval Underwater Systems Center
Newport, RI 02840
Attn: C. N. Pryor
Code 01
(Copy No. 11)

Naval Underwater Systems Center
Attn: D. Goodrich
Code 36315
(Copy No. 12)

Naval Underwater Systems Center
Attn: R. Nadolink
Code 36315
(Copy No. 13)

Naval Underwater Systems Center
Attn: R. Trainor
Code 36314
(Copy No. 14)

Naval Underwater Systems Center
Attn: F. White
Code 36314
(Copy No. 15)

Naval Underwater Systems Center
Attn: Library
Code 54
(Copy No. 16)

Commanding Officer
Naval Ocean Systems Center
San Diego, CA 92152
Attn: J. W. Hoyt
Code 2501
(Copy No. 17)

Naval Ocean Systems Center
Attn: D. Nelson
Code 6342
(Copy No. 18)

Naval Ocean Systems Center
Attn: A. G. Fabula
Code 5311
(Copy No. 19)

DISTRIBUTION LIST FOR UNCLASSIFIED TM 79-18 by J. M. Cimbala, dated
February 2, 1979

Commanding Officer and Director
David W. Taylor Naval Ship R&D Center
Department of the Navy
Bethesda, MD 20084
Attn: W. B. Morgan
Code 154
(Copy No. 20)

David W. Taylor Naval Ship R&D Center
Attn: R. Cumming
Code 1544
(Copy No. 21)

David W. Taylor Naval Ship R&D Center
Attn: T. T. Huang
Code 1552
(Copy No. 22)

David W. Taylor Naval Ship R&D Center
Attn: J. McCarthy
Code 1552
(Copy No. 23)

David W. Taylor Naval Ship R&D Center
Attn: M. M. Sevik
Code 19
(Copy No. 24)

David W. Taylor Naval Ship R&D Center
Attn: Library
Code 522.2
(Copy No. 25)

Commanding Officer and Director
David W. Taylor Naval Ship R&D Center
Department of the Navy
Annapolis Laboratory
Annapolis, MD 21402
Attn: J. G. Stricker
Code 2721
(Copy No. 26)

Commander
Naval Surface Weapon Center
Silver Spring, MD 20910
Attn: G. C. Gaunard
Code R-31
(Copy No. 27)

Naval Surface Weapon Center
Attn: J. L. Baldwin
Code WA-42
(Copy No. 28)

Naval Surface Weapon Center
Attn: W. J. Glowacki
Code R-44
(Copy No. 29)

Office of Naval Research
Department of the Navy
800 N. Quincy Street
Arlington, VA 22217
Attn: R. Cooper
Code 438
(Copy No. 30)

Office of Naval Research
Attn: H. Fitzpatrick
Code 438
(Copy No. 31)

Defense Documentation Center
5010 Duke Street
Cameron Station
Alexandria, VA 22314
(Copies No. 32 to and
including 43)

National Bureau of Standards
Aerodynamics Section
Washington, DC 20234
Attn: P. S. Klebanoff
(Copy No. 44)

Rand Corporation
1700 Main Street
Santa Monica, CA 90406
Attn: C. Gazley
(Copy No. 45)

Jet Propulsion Laboratory
4800 Oak Grove Drive
Pasadena, CA 91103
Attn: Dr. Leslie Mack
(Copy No. 46)

DISTRIBUTION LIST FOR UNCLASSIFIED TM 79-18 by J. M. Cimbala, dated
February 2, 1979

Iowa Institute of Hydraulic Research
The University of Iowa
Iowa City, Iowa 52240
Attn: V. C. Patel
(Copy No. 47)

Dynamics Technology, Inc.
3838 Carson Street, Suite 110
Torrance, CA 90503
Attn: Wayne H. Haigh
(Copy No. 48)

Applied Research Laboratory
The Pennsylvania State University
Post Office Box 30
State College, PA 16801
Attn: J. M. Cimbala
(Copy No. 49)

Applied Research Laboratory
Attn: J. J. Eisenhuth
(Copy No. 50)

Applied Research Laboratory
Attn: R. E. Henderson
(Copy No. 51)

Applied Research Laboratory
Attn: G. H. Hoffman
(Copy No. 52)

Applied Research Laboratory
Attn: B. E. Robbins
(Copy No. 53)

Applied Research Laboratory
Attn: GTWT File
(Copy No. 54)